ETH
Eidgenössische Technische Hochschule Zürich
Swiss Federal Institute of Technology Zurich

Communication Technology Laboratory
Wireless Communications Group

Power Control and Distributed Beamforming for the Relay Carpet

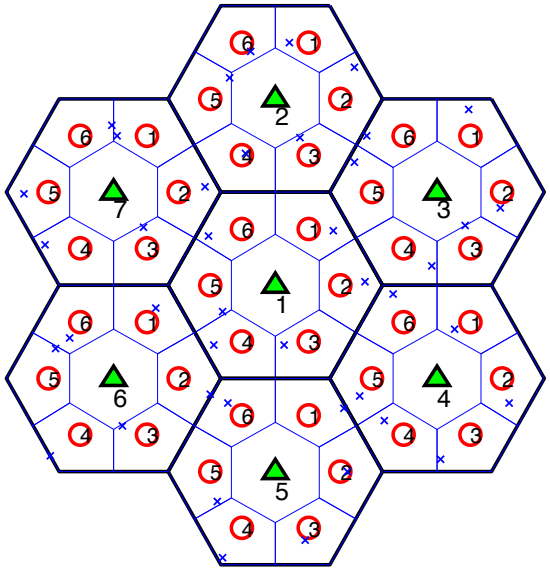

Semester Thesis
Spring 2013

Celestine Dünner

Advisor: Raphael Rolny
Professor: Prof. Dr. Armin Wittneben

Abstract

The increasing demand for ubiquitous high data rates sets high expectations on future cellular networks. To enable these requirements, the Relay Carpet concept is proposed, a two-hop network where few base stations are supported by a large number of relays. If the relays are mounted on fixed positions, the channel from base station to relay can be assumed to be quasi static, whereby CSI estimation for base station cooperation is simplified and the large number of antennas allows to apply multi-user MIMO. Each base station is allocated to one cell and ubiquitous relaying guarantees that all mobiles within the cell can be served by at least one relay in their close vicinity. In this semester thesis, different power control schemes for the promising Relay Carpet concept are developed in order to improve interference management and to reduce noise amplification at the relays. The first power control scheme focuses on minimizing the overall transmit power under a certain rate requirement. In a second implementation, we consider the outage probability as a figure of merit and show that by allocating a fixed total transmit power in a more sophisticated manner, the outage can significantly be decreased. The last objective treated in this thesis is the MaxMin approach, an iterative algorithm that aims to maximize the minimum rate. First, a heuristic algorithm is implemented and then compared to a gradient based algorithm. Finally, performance of these different schemes is discussed based on simulation results.

Preface

This Semester Thesis is part of the graduate study at the Department of Information Technology and Electrical Engineering (D-ITET) at the Swiss Federal Institute of Technology (ETH) Zurich.

The author certifies that this Semester Thesis, and the research to which it refers, are the product of the author's own work, and that any ideas or quotations from the work of other people, published or otherwise, are fully acknowledged in accordance with the standard referring practices of the discipline.

Celestine Dünner

Author:	Celestine Dünner	cduenner@ee.ethz.ch
Advisor:	Raphael Rolny	rolny@nari.ee.ethz.ch
Professor:	Prof. Dr. Armin Wittneben	wittneben@nari.ee.ethz.ch

Contents

List of Figures

List of Tables

List of Algorithms

Chapter 1

Introduction

The rapidly increasing number of mobile devices and the high expectations on throughput and ubiquitous high data rates set high demands on future cellular networks [1]. There are several existing approaches that are developed in order to enable these gains. All of these ideas have advantages but also significant drawbacks. The Relay Carpet concept aims to combine the advantages of different schemes.

One approach is to increase the number of base station antennas which allows to serve multiple users at the same time [2]. An alternative is to build heterogenous networks with small cells [3], in which additional antennas are distributed in space. Both of these approaches can increase the overall throughput of the network. However, individual rates are limited by the small number of mobile antennas and suffer from large interference. A third approach aims for efficient interference management that mitigates or cancels interference. Therefore, base station cooperation, also referred to as coordinated multipoint (CoMP) transmission, can be applied [4], [5]. This brings several challenges. In order to enable base station cooperation, channel state information (CSI) and user data have to be exchanged constantly with the cooperation partners. This causes huge traffic in the network. Moreover, the number of channel coefficient and CSI increases rapidly with the number of antennas. Achievable performance gains might therefore stagnate or even decrease with a growing number of involved antennas [6].

1.1 Relay Carpet Concept

The Relay Carpet concept combines the three approaches explained. Large antenna arrays are used to apply multiuser MIMO strategies for many users and a large number of infrastructure nodes are distributed in order to build small cells. The wide coverage is achieved by spreading a large number of relays across the entire area that support few base stations [7].

That is also where the name Relay Carpet has its origin - the area is covered by the relays like a carpet. Further, each mobile is guaranteed to have a relay available in its vicinity.

Distributed interference management can be achieved by collaboration of base stations as well as relays. Depending on its abilities and the available CSI, each node can contribute to reduce interference within the network. As explained earlier, the need of current CSI causes a huge overhead by channel estimation, and large traffic in the network. This overhead can significantly be reduced by the Relay Carpet concept. The relay stations are mounted on fixed positions, preferably with good connection to their corresponding base station, which leads

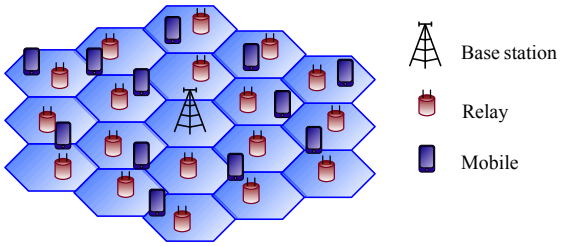

Figure 1.1: The Relay Carpet: A sophisticated BS serves a large number of mobiles in the same physical channel by the help of many distributed relays.

to a slow fading or, depending on the environment, even quasi static channel between base station (BS) and relay station (RS). This simplifies the CSI estimation at the BSs, because there is no need to reestimate the channel constantly. The simplification of the CSI estimation at the BS allows for more sophisticated multiuser MIMO beamforming techniques. From the point of view of each node, the network looks much less complex than the original one. For the mobiles, the network appears similar as a femto cell network, where they are served by small nodes with only few antennas. The relays see an effective channel of reduced dimension from their BS.

1.2 Power Control

A further step for efficient interference management is the implementation of power control schemes. By allocating power at the different transmitting nodes in a sophisticated manner, interference at the remaining nodes can be controlled and reduced [8]. The problem of noise amplification at the relays, which is a main drawback of applying amplify and forward relaying, can be addressed using power control. By identifying little signal and high noise contribution in the received signal, power can systematically be allocated and pure noise amplification can be stopped.

In point to point networks increasing transmit power always results in higher rates. In interference limited networks, however, this is not the case and power control can lead to an overall transmit power reduction and at the same time an increase in rate [9].

Mobiles that have a very good channel to their relays do not need as much transmit signal power as relays that suffer from high interference or bad channel conditions. As the reduction of transmit power brings at the same time an interference reduction in the whole network, saving power can have a beneficial impact on the overall performance. Further, power control can also be applied to aim for specific optimization objectives like maximizing the smallest rate within a cell or focusing on achieving the lowest outage rate possible. Both of these approaches can be achieved by redistributing power within the network in a specific manner and reducing the rate and therewith the power of high rate achieving nodes in favor of the remaining network.

Nevertheless, many challenges and difficulties come with the task of power control, as there is a high unpredictable coupling of parameters. Increasing transmit power and thereby the rate at one node decreases at the same time the rate at other nodes. Also performing joint optimization at the relays and at the base stations can lead to problems. As the optimization

of the BS power allocation can not act improving in rate after relay optimization is done and the optimization objective is already achieved. The challenge of finding approaches that nevertheless guarantee continuous improvement are subject of this thesis.

The potential improvement of the overall performance by implementing sophisticated power control schemes is the motivation for this work. Different power control algorithms aiming for different objectives, that can be applied to different kinds of relays and transmission schemes, are proposed and implemented.

1.3 Thesis Outline

In Chapter 2, an overview of the theoretical knowledge, that is needed to build up the relay carpet model is given and relays are introduced. Then, the Relay Carpet concept is presented. Notation and implementation are introduced and the achievable rate as a performance criterion is derived. This is followed by Chapter 4. This chapter is divided into three parts, capturing three different power control objectives. In these parts, different power control schemes are presented and first tested in a simplified environment. Then, the most promising approaches are extended to be applied to the entire Relay Carpet with multiple cells. Again, simulation results are shown and discussed. In Chapter 5, the elaborated power control schemes are applied to more advanced relays and finally, the thesis is completed by a conclusion that summarizes the knowledge gained on the potential of power control.

Chapter 2

Theory

2.1 Conventional Network

In a conventional network, we have several base stations that are located on fixed positions and there are mobiles that have to be served by these BSs.

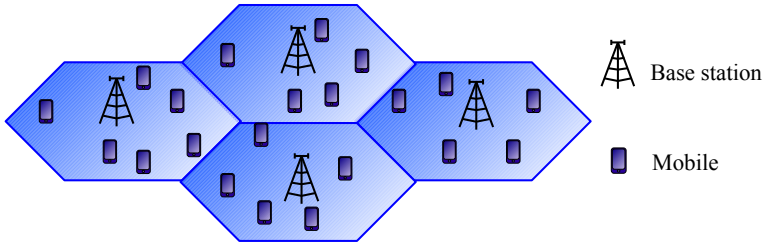

Figure 2.1: Conventional Network: Few base stations serve a large number of mobiles.

Figure 2.1 shows how space is divided into areas. In each area we have one base station and multiple mobiles (MS). One BS is allotted to the mobiles within its area. To derive this multiuser MIMO network, we start by introducing the discrete signal model for the single-input single-output (SISO) case and then extend the model step by step until we have the means to describe the complete network with MIMO nodes.

Throughout the whole thesis we consider only the downlink, which refers to the data transmission from BS to MS.

2.1.1 Discrete Signal Model

The derivations of the discrete signal model are mostly taken from [10]. The transmit signal in Quadrature Amplitude Modulation (QAM) consists of amplitude modulated pulses multiplied by sinusoidal carrier signals. The transmitted data is coded in the symbols a_k and b_k

$$s(t) = \cos(\omega_0 t + \phi_0) \cdot \sum_k a_k g(t - kT) - \sin(\omega_0 t + \phi_0) \cdot \sum_k b_k g(t - kT).$$

Under the assumption that the base pulse $g(t)$ is bandlimited to f_0, i.e. $G(f) = 0 \; \forall |f| >$

f_0, the QAM transmit signal can be expressed without loss of generality by the equivalent baseband signal

$$s_{\mathrm{B}}(t) = e^{j\phi_0} \cdot \left(\sum_k a_k g(t - kT) + j \sum_k b_k g(t - kT) \right) = e^{j\phi_0} \cdot \sum_k s_k g(t - kT),$$

where $s(t) = \mathrm{Re}\{s_{\mathrm{B}}(t) \cdot \exp(j\omega_0 t)\}$ and s_k denotes the complex transmit symbol. The receiver demodulates the QAM signal by performing a down-conversion. This is achieved by multiplying the received signal in one receiver branch with $\cos(\omega_1 t + \phi_1)$ and in the second branch by -$\sin(\omega_1 t + \phi_1)$ and then applying a low pass filter in each branch. Thereby, the $2f_0$ frequency terms are eliminated. In equivalent baseband representation these receiver operations amount to a frequency shift and a phase shift. Let $r_{\mathrm{B}}(t)$ be the equivalent baseband representation of the received signal. After down-conversion we obtain

$$d_{\mathrm{B}}(t) = r_{\mathrm{B}}(t) \cdot e^{j(\omega_0 - \omega_1)t} \cdot e^{j(\phi_0 - \phi_1)}.$$

The receiver then generates sample values of the demodulated signal. These sample values form a sufficient statistic for the transmit symbols, conditioned that the sampling theorem is satisfied and thereby intersymbol interference is eliminated. In AWGN, the detection consists of a matched filter $g_{MF}(t) = g^*(-t)$ followed by T-spaced sampling. The T-spaced transmit symbols are mapped to the output values of the sampler by the following rule:

$$d_k = \sum_m (a_m + jb_m) \cdot h_{k-m} + n_k = \sum_k s_m \cdot h_{k.m} + n_k$$

The filter coeffitients h_k in the discrete symbol spaced signal model capture the impact of all filters in the transmission chain. And n_k denotes the noise samples, where additive white Gaussian noise (AWGN) with two-sided power spectral density $N_0/2$ translates to a complex normal white noise process in equivalent baseband. If the channel is slow fading, which means that the channel is considered to be constant during the time of transmission, the discrete model simplifies to

$$d_k = h \cdot s_k + n_k.$$

Capacity

The channel capacity of the SISO system is given by [11]

$$\mathcal{C} = \log_2(1 + \mathrm{SNR}) = \log_2 \left(1 + \frac{|h|^2 \cdot P_{\mathrm{S}}}{\sigma_{\mathrm{n}}^2} \right) \text{[bit per channel use]}.$$

Here, σ_{n} is the variance of the additive noise and P_{S} the variance of the complex transmit symbols.

2.1.2 MIMO

Transmitters are in general equipped with multiple sending antennas and receivers may also be equipped with more than one receive antenna. M_{S} denotes the number of sender antennas and M_{D} denotes the number of antennas at the destination. The source wants to transmit $d_{\mathrm{s}} \leq \min(M_{\mathrm{D}}, M_{\mathrm{S}})$ data streams to the destination.

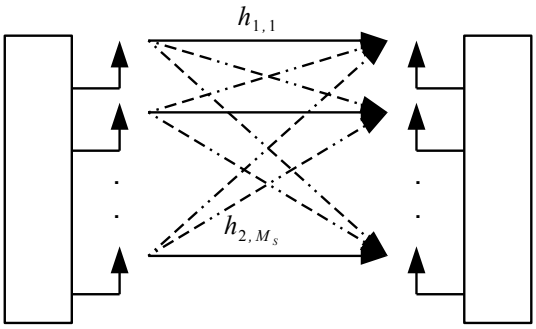

Figure 2.2: Multiple antenna array.

In order to take advantage of the multiple antennas, the sender can multiply the transmit signal first by the beamforming matrix $\mathbf{Q} \in \mathbb{C}^{M_{\mathrm{S}} \mathrm{x}\, d_{\mathrm{s}}}$ and then transmits the premultiplied signal to the receiver. At the destination, the signal

$$\mathbf{y} = \mathbf{HQs} + \mathbf{n}$$

is received. The channel matrix $\mathbf{H} \in \mathbb{C}^{M_{\mathrm{D}} \mathrm{x} M_{\mathrm{S}}}$ captures the channel coefficients, entry $[\mathbf{H}]_{i,j}$ describes the channel between source antenna j and destination antenna i.

MIMO Capacity via SVD

The capacity of a single source destination pair equipped with multiple antennas transmitting over an AWGN channel is given by [12] :

$$C = \max_{\mathbf{Q}:\mathrm{Tr}\{\mathbf{QQ}^H\} \leq P} \log_2 \det(\mathbf{I} + \frac{1}{\sigma_{\mathrm{n}}^2} \mathbf{HQQ}^H \mathbf{H}^H).$$

We assume the entries of the transmit signal $\mathbf{s} \in \mathbb{C}^{d_{\mathrm{s}}}$ to be taken from an i.i.d. Gaussian code book $\mathbf{s} \sim \mathcal{CN}(\mathbf{0}, \mathbf{I})$ and the noise $\mathbf{n} \sim \mathcal{CN}(\mathbf{0}, \sigma_{\mathrm{n}}^2 \mathbf{I})$ to be complex white Gaussian noise. The beamforming matrix $\mathbf{Q}$ that is capacity achieving can be derived by decomposing the vector channel into a set of parallel, independent scalar Gaussian subchannels. Therefore, we decompose the channel matrix $\mathbf{H}$ according to the singular value decomposition (SVD) into $\mathbf{H} = \mathbf{UDV}^H$ where $\mathbf{D}$ is a rectangular matrix with the singular values of the channel $\lambda_1 \geq \lambda_2 \geq ... \geq \lambda_p$ on its diagonal and $\mathbf{U}$ and $\mathbf{V}$ are unitary matrices. In case of perfect CSI, the channel information can be used at the base station to define the beamforming matrix $\mathbf{Q} = \mathbf{VP}$, where $\mathbf{P}$ is a diagonal matrix, and at the receiver to get the transformed received signal

$$\widetilde{\mathbf{y}} = \mathbf{U}^H \mathbf{y} = \mathbf{U}^H \mathbf{HQs} = \mathbf{U}^H \mathbf{UDV}^H \mathbf{VPs} = \mathbf{DPs}.$$

Hence, the channels are orthogonalized and we have an equivalent representation as a parallel Gaussian channel, where capacity is known. The received signal vector is given by

$$\widetilde{\mathbf{y}} = \begin{bmatrix} \lambda_1 s_1 + n_1 \\ ... \\ \lambda_{\mathrm{p}} s_p + n_p \end{bmatrix}, \tag{2.1}$$

where λ_i are the eigenmodes of the channel.

What remains is to choose the diagonal values P_i of $\mathbf{P}$ such that $\mathbf{Q} = \mathbf{VP}$ is optimal. The solution to this maximization problem is to choose waterfilling power allocations for P_i, that satisfy the sum power constraint.

Waterfilling

The waterfilling (WF) power allocation is the solution to the optimization problem of maximizing the sum rate at the receivers [9]. More power is allocated to the better subchannels with higher signal-to-noise ratios (SNR), such that the total sum data rate is maximized. Waterfilling is performed at the transmitter by multiplying the beamforming matrix by the waterfilling matrix $\mathbf{P}$, with the power allocations on its diagonal.

We consider the optimization problem

$$\begin{aligned} \underset{P_0,\ldots,P_{N-1}}{\text{maximize}} \quad & \sum_{i=0}^{N-1} \log\left(1 + \frac{P_i \lambda_i^2}{\sigma_{\mathrm{n}}^2}\right) \\ \text{subject to:} \quad & \sum_{i=1}^{N-1} P_i \leq P. \end{aligned}$$

The optimal power allocation can explicitly be found. The objective function is concave in P_i and therefore, the problem can be solved by the Lagrangian method. The Lagrangian can be written as a function of the Lagrange multiplier ν and the eigenmodes λ_i of the channel, as in (2.1):

$$\mathcal{L}(\lambda, P_0, ..., P_{N-1}) = \sum_{i=0}^{N-1} \log\left(1 + \frac{P_i \lambda_i^2}{\sigma_{\mathrm{n}}^2}\right) - \nu \sum_{i=0}^{N-1} P_i.$$

The Kuhn-Tucker condition for the optimal solution of a maximization problem is

$$\frac{\partial \mathcal{L}}{\partial P_i} \begin{cases} = 0 & \text{if } P_i > 0 \\ \leq 0 & \text{if } P_i = 0 \end{cases}.$$

These conditions are satisfied by the power allocation

$$P_i = \left(\nu - \frac{\sigma_{\mathrm{n}}^2}{\lambda_i^2}\right)^+.$$

This power allocation is therefore optimal, where $x^+ = \max(x, 0)$. The Lagrange multiplier ν is chosen such that the sum power constraint is met.

The resulting power allocation can be illustrated by filling water into a vessel, as can be seen in Figure 2.4. The values $\frac{\sigma_{\mathrm{n}}^2}{\lambda_i^2}$ are plotted as a function of the subcarrier index $n = 0, ..., N$, as tracing out the bottom of a vessel. Then P units of water are filled into the vessel, the depth of the water at subcarrier n is the power allocated to that subcarrier and the value ν is the height of the water surface. Thus this optimal strategy is called *waterfilling*.

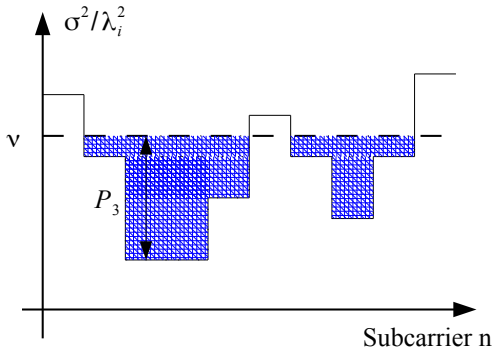

Figure 2.3: Waterfilling power allocation over N subcarriers.

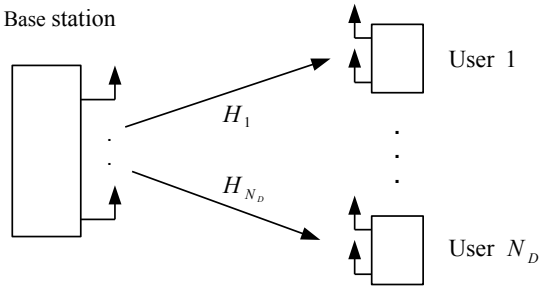

Figure 2.4: One BS serves N_D users simultaneously in the same physical channel.

2.1.3 Multiuser MIMO

In this section, the MIMO model derived in the last chapter is extended to the multiuser case. As a base station serves many users at the same time, we now consider the case where we have N_D users that are served by one base station. The base station simultaneously transmits multiple signals s_i that are intended for different users. Thereby, the problem of interference occurs. At user k, the signal

$$\mathbf{y}_k = \sum_{i=1}^{N_\mathrm{D}} \mathbf{H}_k \mathbf{Q}_i \mathbf{s}_i + \mathbf{n}_k \tag{2.2}$$

is received, where $\mathbf{H}_k$ captures the channel between the BS and receiver k. The term s_k describes the signal intended for receiver k and the other summands for $i \neq k$ are not desired and cause interference. This interference can be controlled by premultiplying the transmit signal $\mathbf{s}_i$ by the linear precoding matrix $\mathbf{Q}_i$ before transmission. This strategy is called beamforming. $\mathbf{Q}$ can be designed to achieve beneficial interference patterns.

The capacity of such a network can be achieved by dirty paper coding [13]. This non-linear precoding scheme is, however, difficult to implement in practice. To this end, we focus on linear schemes such as zero-forcing, presented in the next section.

Block Zero Forcing

Zero forcing (ZF) is a beamforming strategy that is applied in multiuser networks in order to eliminate interference at the receivers [14]. If the transmitter knows the downlink CSI perfectly, zero forcing can achieve capacity at the limit SNR $\to \infty$. The signals transmitted by the sender are precoded in such a way that the signals do not interfere at the receivers, in other words, the signal component alotted to one receiver vanishes at all the other nodes and thereby interference is avoided. The minimum number of transmit antennas needed to guarantee this is $M_{\mathrm{S}} \geq N_{\mathrm{D}} \cdot M_{\mathrm{D}}$.

In (2.2) we found the received signal at receiver k for the multiuser network to be

$$\mathbf{y}_k = \sum_{i=1}^{N_{\mathrm{D}}} \mathbf{H}_k \mathbf{Q}_i \mathbf{s}_i + \mathbf{n}_k$$

The multiplication of $\mathbf{s}_i$ by the beamforming matrix $\mathbf{Q}_i$, denoted by $\mathbf{Z}_i$ in case of zero-forcing, should result in the desired interference pattern. To achieve zeroforcing the precoding matrix $\mathbf{Z}_i$ is chosen to be orthogonal to all channels causing interference.

$$\mathbf{Z}_i = \mathrm{null}\left\{ \left[\mathbf{H}_1{}^{\mathrm{T}}, ..., \mathbf{H}_{i-1}{}^{\mathrm{T}}, \mathbf{H}_{i+1}{}^{\mathrm{T}}, ..., \mathbf{H}_{N_{\mathrm{D}}}{}^{\mathrm{T}} \right]^{\mathrm{T}} \right\}$$

spans the space in which $\mathbf{H}_i \cdot \mathbf{Q}_k = \mathbf{0}$, for $i \neq k$, is ensured. Recall that $\mathbf{H}_i$ denotes the channel between the base station and receiver i. Hence, receiver k receives the signal

$$\mathbf{y}_k = \mathbf{H}_k \cdot \mathbf{Z}_k \cdot \mathbf{s}_k + \mathbf{n}_k,$$

as all the other summands $\mathbf{H}_i \cdot \mathbf{Z}_k \cdot \mathbf{s}_k$ where $i \neq k$ are zero. Interference free transmission is achieved and the receiver only has to deal with the noise term $\mathbf{n}$.

2.1.4 Multiple Source Destination Pairs

We are now considering the case where we have N source destination pairs that are all exchanging data streams simultaneously as illustrated in Figure 2.5. As we again have multiple signals that are transmitted through a shared medium we have to be aware that the transmission of one BS causes interference at all other receivers.

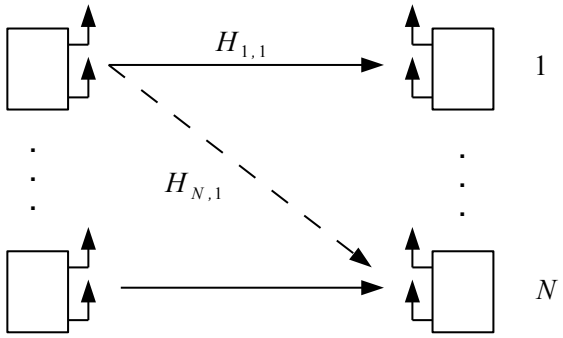

Figure 2.5: Multiple source destination pairs are exchanging data bit streams simultaneously.

The received signals at destination i

$$\mathbf{y}_i = \sum_{k=1}^{N} \mathbf{H}_{i,k} \cdot \mathbf{Q}_k \cdot \mathbf{s}_k + \mathbf{n}_i$$

is the superposition of the independent transmit signal coming from different base stations. The channel matrix $\mathbf{H}_{i,j} \in \mathbb{C}^{M_\mathrm{D} \mathrm{x} M_\mathrm{S}}$ captures the channel coeffitients between source j and destination i. $\mathbf{Q}_k$ denotes the precoding matrix at transmitting node k.

Achievable Rate

For MIMO multi-user channels, the capacity is in general not known exactly. Therefore we consider for comparison only achievable rates, which are a lower bound to the capacity. The achievable rate is a reference value that is known to lie within the capacity region, but the distance to capacity is not exactly known. For given precoding matrices and zero cross-correlation between noise and transmit signal, the rate

$$R_k = \log_2 \det \left(\mathbf{I} + \left(\mathbf{K}_\mathrm{n}^{(k)} + \mathbf{K}_\mathrm{i}^{(k)} \right)^{-1} \cdot \mathbf{K}_\mathrm{s}^{(k)} \right)$$

is achievable and a function of the desired signal covariance matrix

$$\mathbf{K}_\mathrm{s}^{(k)} = \mathbf{H}_{k,k} \mathbf{Q}_k \mathrm{E}\left[\mathbf{s}_k \mathbf{s}_k^H \right] \mathbf{Q}_k^H \mathbf{H}_{k,k}^H$$

and the inverse of the noise and interference covariance matrix

$$\mathbf{K}_\mathrm{i}^{(k)} = \sum_{\substack{i=1 \\ i \neq k}}^{N_\mathrm{D}} \sum_{\substack{j=1 \\ j \neq k}}^{N_\mathrm{D}} \mathbf{H}_{k,i} \mathbf{Q}_i \mathrm{E}\left[\mathbf{s}_i \mathbf{s}_j^H \right] \mathbf{Q}_j^H \mathbf{H}_{k,j}^H,$$

$$\mathbf{K}_\mathrm{n}^{(k)} = \sigma_\mathrm{n}^2 \mathbf{I}.$$

We assume independent transmit signals. Hence, the expression for $\mathbf{K}_\mathrm{i}$ can be simplified, using $\mathrm{E}\left[\mathbf{s}_i \mathbf{s}_k^H \right] = \mathbf{0}$ for $i \neq k$, to

$$\mathbf{K}_\mathrm{i}^{(k)} = \sum_{\substack{i=1 \\ i \neq k}}^{N_\mathrm{D}} \mathbf{H}_{k,i} \mathbf{Q}_i \mathrm{E}\left[\mathbf{s}_i \mathbf{s}_i^H \right] \mathbf{Q}_i^H \mathbf{H}_{k,i}^H.$$

So far, we have built a network consisting of multiple transmitters and multiple receivers equipped with several antennas. In the next step, this conventional network is extended to the case where multiple relays assist the communication between source and destionation. Therefore relaying is introduced first and then the Relay Carpet concept is built up step by step.

2.2 Relaying

Contents of this section are partly taken from [10].
In relaying, we have additional nodes (relays) supporting the exchange of information bit streams between source and destination pairs. The relays assist the communication without transmitting own information bit streams. There are different kinds of relays that differ by their complexity and their mode of operation.

2.2.1 Relay Classification

On one hand we distinguish between half and full duplex relays. Full duplex relays can receive and transmit simultaneously in the same physical channel. This requires a very high isolation of transmitter and receiver branch, as in wireless links the received signals can differ by as much as 120dB. In contrast to full duplex relays, half duplex relays are in turn either in receive or in transmit mode. Half duplex relays can either implement time division duplexing (TDD) or frequency division duplexing (FDD). In TDD outward and return signals are separated by time division multiplexing whereas in FDD the separation is achieved by transmitter and receiver operating in different frequency bands. Thus the transmission of one symbol from source to destination via relay involves two time slots using TDD and twice the bandwidth using FDD. This loss in spectral efficiency of 50% can partially be recovered by an approach called two-way relaying [15]. Further, we distinguish between different modes of operation. The simplest approach is Amplify and Forward (AF) Relaying. AF relays just amplify the received signal and retransmit it, this is equivalent to multiplying the received signal by a relay gain matrix in the equivalent base band. A different approach is Decode and Forward (DF) Relaying. This approach improves the main disadvantage of AF relaying, which is that not only the desired signal, but also noise is amplified and retransmitted at the relays. This results in amplified noise propagating through the network and being received at the destination. DF relays are completely decoding and reencoding the signal before retransmission. In this way, noise can be removed and does not appear at the destination. However, DF relaying networks suffer from error propagation. There exist further kinds of relays, but they are not discussed here.

2.2.2 Single AF Relay Network

The link between source and destination is supported by one AF relay with M_{R} antennas. As the direct link between source and destination is ignored for further considerations, the relay turns the link into a two-hop link. In a first hop, information is sent from the source to the relay and in a second hop, the data is sent from the relay to the destination.

The source wants to transmit d_{s} data streams to the destination via the relay. The received signal at the relay, ignoring the direct path,

$$\mathbf{y}^{(\mathrm{R})} = \mathbf{H} \cdot \mathbf{Q} \cdot \mathbf{s} + \mathbf{n}$$

is the premultiplied source signal $\mathbf{s} \in \mathbb{C}^{d_{\mathrm{s}}}$ transmitted over the source-relay channel $\mathbf{H} \in \mathbb{C}^{M_{\mathrm{R}} \mathrm{x} M_{\mathrm{S}}}$, disturbed by additive complex white Gaussian noise. The AF relay multiplies the received signal by the relay gain matrix $\mathbf{G} \in \mathbb{C}^{M_{\mathrm{R}} \mathrm{x} M_{\mathrm{R}}}$ and then forwards it to the destination. At the destination, the signal

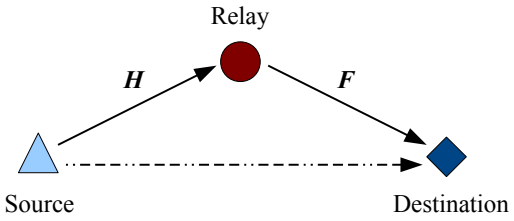

Figure 2.6: Data transmission via a single relay.

$$\mathbf{d} = \mathbf{FG} \cdot (\mathbf{HQs} + \mathbf{n}) + \mathbf{w} = \mathbf{FGHQs} + (\mathbf{FGn} + \mathbf{w})$$

is received, where the channel matrix $\mathbf{F} \in \mathbb{C}^{M_{\mathrm{R}} \mathrm{x} M_{\mathrm{D}}}$ describes the channel between relay and destination. The noise terms at the destination as well as at the relay, are assumed to be independent white and Gaussian, denoted by $\mathbf{w} \sim \mathcal{CN}(\mathbf{0}, \sigma_{\mathrm{w}}^2 \mathbf{I})$ and $\mathbf{n} \sim \mathcal{CN}(\mathbf{0}, \sigma_{\mathrm{n}}^2 \mathbf{I})$

The signal covariance matrix

$$\mathbf{K}_{\mathrm{s}} = \mathrm{E}\left[(\mathbf{FGHQs}) \cdot (\mathbf{FGHQs})^H\right] = \mathbf{FGHQ} \cdot \mathrm{E}\left[\mathbf{ss}^H\right] \mathbf{Q}^H \mathbf{H}^H \mathbf{G}^H \mathbf{F}^H$$

and the noise covariance matrix at the receiver

$$\mathbf{K}_{\mathrm{n}} = \mathrm{E}\left[(\mathbf{F} \cdot \mathbf{G} \cdot \mathbf{n} + \mathbf{w}) \cdot (\mathbf{F} \cdot \mathbf{G} \cdot \mathbf{n} + \mathbf{w})^H\right] = \mathbf{F} \cdot \mathbf{G} \cdot \mathbf{G}^H \cdot \mathbf{F}^H \sigma_{\mathrm{n}}^2 + \sigma_{\mathrm{w}}^2 \mathbf{I}$$

determine the achievable rate

$$R = \frac{1}{2} \cdot \log_2 \det\left(\mathbf{I} + \mathbf{K}_{\mathrm{n}}^{-1} \cdot \mathbf{K}_{\mathrm{s}}\right).$$

By combining the knowledge gained from building up the conventional network and the consideration of the AF relay link, the Relay Carpet network model can be built up. In the next chapter, the Relay Carpet is introduced whereby we restrict ourselves to AF relays.

Chapter 3

Relay Carpet

The concept of the Relay Carpet aims to increase coverage, spectral efficiency and to lower power. The basic organization of the network is the same as in a conventional cellular network with micro cells. The area of coverage is partitioned in geographically separated regions, called cells. One base station is placed in each of these regions and serves N_{M} mobiles via N_{R} relays within the region. We assume $N_{\mathrm{R}} = N_{\mathrm{M}}$, which means that each mobile is allocated to one of the relay stations and each relay station serves one mobile. For notational simplicity, the number of mobiles in each cell is the same and the number of antennas is equal for nodes of the same kind. We assume AF relays for this thesis if not stated differently. Hence, the relay amplifies and forwards the received signal coming form the base station to the corresponding mobile station, where the corresponding mobile is always the mobile that is located closest to the relay.

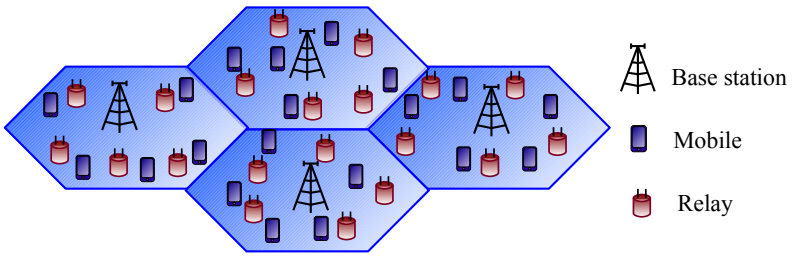

Figure 3.1: Illustration of the Relay Carpet concept.

This concept of distributing multiple relays within the area of one base station has multiple advantages. On one hand, the number of antennas in the network is increased and offers the possibility of spatial multiplexing. Further, the position of the relays is fixed, whereby the channel $\mathbf{H}$ between base station and relay can be assumed to be almost static. Hence, the channel is not needed to be reestimated constantly, which results in a significant decrease in complexity. Another plus factor is the small distance between relay and mobile. Due to the short link, the power of the relays can be kept low and at the same time interference is reduced.

In Figure 3.2 the relay network model is illustrated. The model shows the simplified network for $N_{\mathrm{B}} = 2$ cells of which each contains $N_{\mathrm{R}} = 2$ relays and $N_{\mathrm{M}} = N_{\mathrm{R}}$ mobiles. The cells and the appropriate BS are numbered from 1 to N_{B}. The relay stations are identified

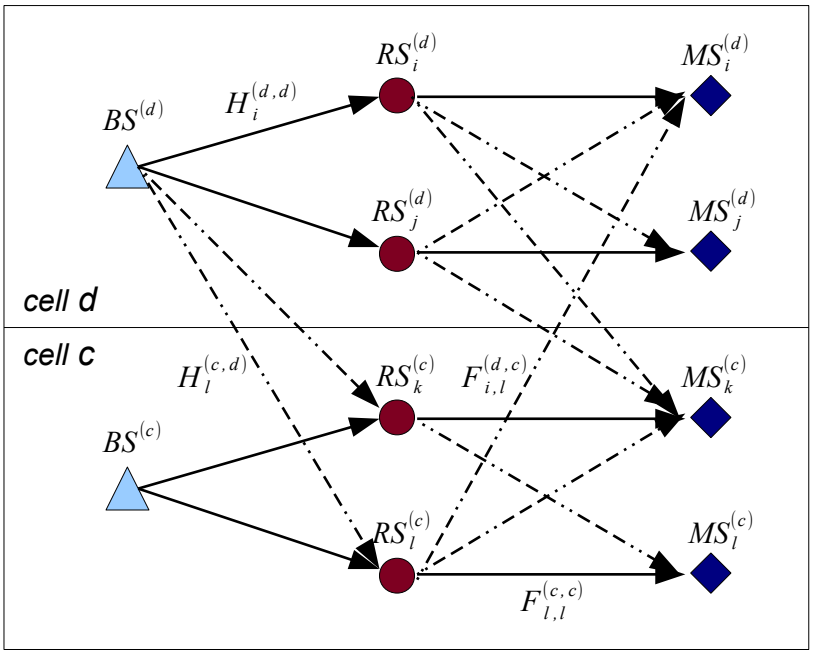

Figure 3.2: Abstraction of the Relay Carpet system model.

by the index of the cell, in the superscript, and the index of the relay within the cell in the subscript, i.e. $\mathrm{RS}_k^{(c)}$ denotes relay k in cell c. The mobile stations are indexed similarly, by the cell index and the index of the mobile within the cell. The channel between the base station $\mathrm{BS}^{(d)}$ and the relay station $\mathrm{RS}_l^{(c)}$ is denoted by the channel matrix $\mathbf{H}_l^{(c,d)} \in \mathbb{C}^{M_\mathrm{R} \mathrm{x} M_\mathrm{B}}$, where M_B denotes the number of base station antennas and M_R the number of antennas of one relay station. The channel matrix $\mathbf{F}_{i,l}^{(d,c)}$ characterizes the channel from $\mathrm{RS}_l^{(c)}$ to $\mathrm{MS}_i^{(d)}$ and is of dimension M_M xM_R.

For the relaying network, we assume that there is no line of sight (LOS) between the base stations and the mobiles. This assumption is appropriate for the urban environment as there are high buildings and blocks making LOS connection impossible. The whole setup is uniquely determined by the channel matrices $\mathbf{F}$ and $\mathbf{H}$, that depend on the position of the relays and the mobiles.

The base stations transmit symbols taken from a i.i.d circular-symmetric Gaussian codebook, $\mathbf{s} \sim \mathcal{CN}(\mathbf{0}, \mathbf{I})$, premultiplied by the beamforming matrix $\mathbf{Q}$. At the $\mathrm{RS}_k^{(c)}$, for $k \in \{1, ...N_\mathrm{R}\}$ and $c \in \{1, ...N_\mathrm{B}\}$, the signal

$$\mathbf{y}_{c,k}^{(\mathrm{R})} = \sum_{d=1}^{N_\mathrm{B}} \mathbf{H}_k^{(c,d)} \cdot \underbrace{\sum_{i=1}^{N_\mathrm{M}} \mathbf{Q}_{d,i} \cdot \mathbf{s}_{d,i}}_{\mathbf{x}_c^{(\mathrm{B})}} + \mathbf{n}_{c,k}$$

is received, where $\mathbf{x}_c^{(\mathrm{B})}$ denotes the transmit signal at $\mathrm{BS}^{(c)}$. As we focus on AF relays, the relay then amplifies the received signal by multiplying it with the relay gain matrix $\mathbf{G}$ and forwards

$$\mathbf{x}_{c,k}^{(\mathrm{R})} = \mathbf{G}_{c,k} \cdot \mathbf{y}_{c,k}^{(\mathrm{R})}.$$

At mobile station $\mathrm{MS}_c^{(k)}$ the signal

$$\begin{aligned}\mathbf{y}_{c,k}^{(\mathrm{M})} &= \sum_{d=1}^{N_\mathrm{B}}\sum_{j=1}^{N_R}\mathbf{F}_{k,j}^{(c,d)}\cdot\mathbf{x}_{d,j}^{(\mathrm{R})}+\mathbf{w}_{c,k}\\ &= \underbrace{\sum_{d=1}^{N_\mathrm{B}}\sum_{j=1}^{N_\mathrm{R}}\sum_{b=1}^{N_\mathrm{B}}\sum_{i=1}^{N_\mathrm{M}}\mathbf{F}_{k,j}^{(c,d)}\mathbf{G}_{d,j}\mathbf{H}_j^{(d,b)}\mathbf{Q}_{b,i}\mathbf{s}_{b,i}}_{\text{base stations}}+\underbrace{\sum_{b=1}^{N_\mathrm{B}}\sum_{j=1}^{N_\mathrm{R}}\mathbf{F}_{k,j}^{(c,d)}\mathbf{G}_{d,j}\mathbf{n}_{d,j}}_{\text{relay noise}}+\underbrace{\mathbf{w}_{c,k}}_{\text{mobile noise}}\end{aligned}$$

is received. The first summand captures signals coming from all different base stations, the second summand captures the amplified noise at the relays that propagates through the network to the MS and the third term describes noise at the MS. The only desired signal component at $\mathrm{MS}_k^{(c)}$ is

$$\sum_{d=1}^{N_\mathrm{B}}\sum_{j=1}^{N_\mathrm{R}}\mathbf{F}_{k,j}^{(c,d)}\mathbf{G}_{d,j}\mathbf{H}_j^{(d,c)}\mathbf{Q}_{c,k}\mathbf{s}_{c,k}$$

and the rest is caused by interference and noise.

Further, we have a power constraint at the base station

$$\left\|\mathbf{x}_c^{(\mathrm{B})}\right\|^2=\sum_{k=1}^{N_\mathrm{M}}\mathrm{Tr}\left\{\mathbf{Q}_{c,k}{\mathbf{Q}_{c,k}}^H\right\}\le P_\mathrm{BS},$$

which reduces to a condition on the beamforming matrix $\mathbf{Q}$. The power constraint at the relay is

$$\mathrm{Tr}\left\{\mathbf{G}_{c,k}\cdot\mathrm{E}\left[\mathbf{y}_{c,k}^{(\mathrm{R})}\cdot{\mathbf{y}_{c,k}^{(\mathrm{R})}}^H\right]\cdot{\mathbf{G}_{c,k}}^H\right\}\le P_\mathrm{RS}.$$

Having derived the expressions for the received signal at the mobile station we consider the achievable rate for the Relay Carpet system in the next section.

3.1 Achievable Rate

Once precoding and relay matrices are chosen, the achievable rate for the downlink channel can be formulated. The downlink rate for the transmission from BS_c to $\mathrm{MS}_k^{(c)}$ in the case of AF relaying is given by

$$R_{c,k}=\log_2\det\left(\mathbf{I}+\left(\mathbf{K}_\mathrm{n}^{(c,k)}+\mathbf{K}_\mathrm{i}^{(c,k)}\right)^{-1}\cdot\mathbf{K}_\mathrm{s}^{(c,k)}\right)\tag{3.1}$$

with the covariance matrix of the desired signal $\mathbf{K}_\mathrm{s}$, interference $\mathbf{K}_\mathrm{i}$ and noise $\mathbf{K}_\mathrm{n}$ given by

$$K_{\mathrm{s}}^{(c,k)} = \sum_{d=1}^{N_{\mathrm{B}}} \sum_{j=1}^{N_{\mathrm{R}}} \sum_{d'=1}^{N_{\mathrm{B}}} \sum_{j'=1}^{N_{\mathrm{M}}} \mathbf{F}_{k,j}^{(c,d)} \mathbf{G}_{d,j} \mathbf{H}_{j}^{(d,c)} \mathbf{Q}_{c,k} \mathbf{Q}_{c,k}{}^{H} \mathbf{H}_{j'}^{(d',c)\,H} \mathbf{G}_{d',j'}^{H} \mathbf{F}_{k,j'}^{(c,d')\,H} \tag{3.2}$$

$$K_{\mathrm{i}}^{(c,k)} = \sum_{b=1}^{N_{\mathrm{B}}} \sum_{\substack{i=1 \\ i \neq k}}^{N_{\mathrm{R}}} \sum_{d=1}^{N_{\mathrm{B}}} \sum_{j=1}^{N_{\mathrm{R}}} \sum_{d'=1}^{N_{\mathrm{B}}} \sum_{j'=1}^{N_{\mathrm{R}}} \mathbf{F}_{k,i}^{(c,d)} \mathbf{G}_{d,j} \mathbf{H}_{j}^{(d,b)} \mathbf{Q}_{b,i} \mathbf{Q}_{b,i}^{H} \mathbf{H}_{j'}^{(d',b)\,H} \mathbf{G}_{d,j'}^{H} \mathbf{F}_{k,j'}^{(c,d')\,H} \tag{3.3}$$

$$K_{\mathrm{n}}^{(c,k)} = \sum_{d=1}^{N_{\mathrm{B}}} \sum_{j=1}^{N_{\mathrm{R}}} \sum_{d'=1}^{N_{\mathrm{B}}} \sum_{j'=1}^{N_{\mathrm{R}}} \mathbf{F}_{k,j}^{(c,d)} \mathbf{G}_{d,j} \sigma_{\mathrm{n}}^2 \mathbf{G}_{d',j'}^{H} \mathbf{F}_{k,j'}^{(c,d')} + \sigma_{\mathrm{w}}^2 \mathbf{I} \tag{3.4}$$

or equivalently

$$K_{\mathrm{i+n}}^{(c,k)} = \mathrm{E}\left[\mathbf{y}_{c,k}^{(\mathrm{M})} \mathbf{y}_{c,k}^{(\mathrm{M})\,H} \right] - K_{\mathrm{s}}^{(c,k)}.$$

For comparison reason we neglect the prelog factor of $\frac{1}{2}$ that comes from the spectral efficiency loss using half duplex relays.

3.2 Sample Implementation

An example implementation used for simulations in this thesis is described in this section and illustrated in Figure 3.3. The network consists of $N_{\mathrm{B}} = 7$ hexagonal cells, in each cell $N_{\mathrm{R}} = 6$ relays are placed on fix positions on a circle around the BS. The position of the $N_{\mathrm{M}} = 6$ mobiles is randomly chosen within a small hexagonal area around the relays. The base stations are equipped with $M_{\mathrm{B}} = 24$, the relays with $M_{\mathrm{R}} = 6$ and the mobiles with $M_{\mathrm{M}} = 2$ antennas. The cells are labeled by numbers $n \in \{1, ...7\}$, the cell in the center is defined to be cell 1 and the adjacent cells are increasingly numbered in clock wise manner starting on the top in the middle. The relays within each cell are also numbered in clockwise fashion starting in the upper right corner of the cell. The channel matrices $\mathbf{H}$ and $\mathbf{F}$ are chosen based on the WINNER II channel model under the assumption of frequency flat block fading. This model performs path loss calculation based on the distance between the nodes and applies the Rice fading channel model with appropriate coefficients in order to realistically model an urban environment. Thereby, high reflections and shadowing is taken into account. The assumption of no LOS is captured by setting the Rician factor, that captures the ratio of signal power in the dominant component, i.e. the direct LOS connection, over the local mean scattered power, is set to zero. Ignoring the LOS turns the Rice fading model into a Rayleigh fading model. More details on the Rayleigh fading model can be found in [16]. If not stated otherwise, the transmit powers are chosen to be 40 W at the base stations and 6W at the relays. The noise variances are $5 \cdot 10^{-12}$ W at the relays as well as at the mobiles.

Figure 3.4 shows a comparison of rates achieved in the conventional network and the Relay Carpet network using the sample implementation described above. It illustrates the improvement in rate that can be achieved by the relay carpet concept. The empirical cumulative distribution function (CDF) of the achievable sum rate arises from simulating more than 1000 different network constellations and will be often used for performance analysis in the following chapters.

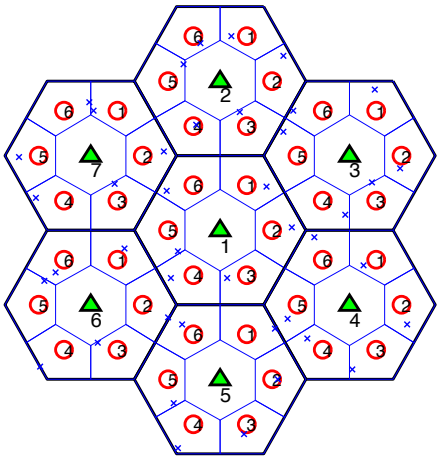

Figure 3.3: Sample Implementation of the Relay Carpet: Cells are numbered, base stations indicated by triangles, relays by red cycles and mobiles by blue crosses.

The blue curve shows the achievable sum rate in the conventional network where base stations perform zero forcing. The red curve shows the result for the Relay Carpet where only the base station performs beamforming on the mobiles, namely zero forcing, and the relays are spatially white. The third green curve shows the results for the case where we have more sophisticated beamforming strategies at the AF relays, which are discussed later in Chapter 5.

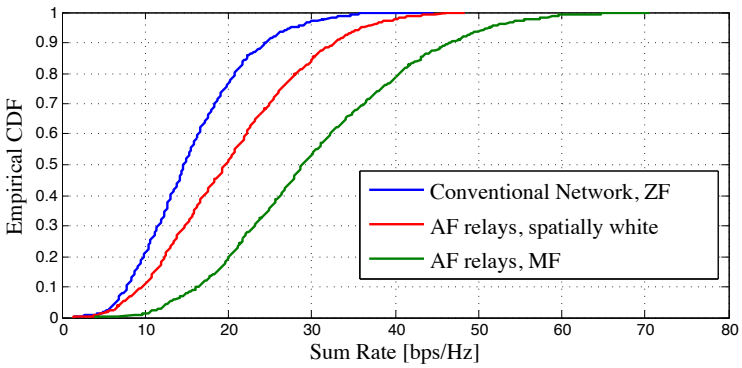

Figure 3.4: CDF of achievable sum rates in conventional and relay networks. The transmit powers are $P_b = 40$ W, $P_r = 6$ W and the noise variance $\sigma_n^2 = 5 \cdot 10^{-12} W$ per 100 MHz bandwidth.

These promising results are motivation to improve the Relay Carpet network by adding additional features. In the following chapters, the Relay Carpet network is extended by different power control schemes that allow further improvements in performance.

Chapter 4

Power Control

Without power control, all senders are forced to transmit signals at a given fixed transmit power. This conventional approach is suboptimal in terms of power consumption and offers possibilities in improvement concerning the achievable rate and the outage probability. As the network is interference limited, a different transmit power allocation, consuming less power may result in better performance. Further, fixed transmit power results in a wide spread in rates that are achieved at the receiver. Some of these rates are unnecessarily high and others uselessly small. These achievable rates depend on the position of the receiver and the different channels between sender and receiver, but also on the interference caused by other senders. Different goals of power control are formulated and elaborated in this chapter. An overview of different power control schemes applicable in wireless cellular networks can be found in [8]. Theses standard schemes, however, can not be applied to the Relay Carpet, as relays and BSs prevent each other from convergence. Therefore, different algorithms are needed and elaboraborated in this chapter for three different objectives.

The first objective is to minimize the overall transmit power by defining a target rate, that is to be achieved at all mobiles. Reducing power at relays that result in achievable rates higher than the target rate, leads to reduced interference at the remaining mobiles. By taking advantage of this fact, an optimal power allocation in the sense of power consumption is elaborated. A second optimization goal is to maximize the minimum achievable rate per cell. This is performed on the condition that the sum transmit power is kept constant. A fixed total amount of power is redistributed in such a way, that all mobiles achieve the same rate and no relay power can be reduced in favor of an other smaller rate. A third optimization goal is to minimize the outage probability of single relays by keeping the overall sum transmit power constant. An algorithm that goes for this goal is developed in Section 4.4. In the following sections, first, it is explained how parameters are influenced in order to perform power control and then, iterative algorithms that implement the different optimization objectives introduced are presented.

4.1 Controllable Parameters

In order to perform power control, the two parameters, base station transmit power and relay transmit power, can be influenced.

4.1.1 Relay Transmit Power

The transmit power of each relay can be adapted by adjusting the relay precoding matrix. As we first consider spatially white AF relays, the relay gain matrix is equal to the scaled identity matrix $\mathbf{G}_{c,i} = \beta_{c,i} \cdot \mathbf{I}$. In this case, the relay transmit power can directly be controlled by individually choosing an appropriate scaling factor

$$\beta_{c,i} = \sqrt{\frac{P_{\mathrm{RS}_i^{(c)}}}{\mathrm{Tr}\left\{\mathrm{E}\left[\mathbf{y}_{c,i}^{(\mathrm{R})}\mathbf{y}_{c,i}^{(\mathrm{R})H}\right]\right\}}} \tag{4.1}$$

for each relay. The denominator in (5.1) describes the actual power of the receive signal at the relay and $\mathrm{P}_{\mathrm{RS}_i^{(c)}}$ the desired transmit power of relay $\mathrm{RS}_i^{(c)}$.

4.1.2 Base Station Transmit Power

The base station transmit power for each relay within one cell can individually be assigned. The base stations are performing beamforming (BF) which is achieved by multiplying the transmit signal intended for $\mathrm{RS}_k^{(c)}$ by the precoding matrix $\mathbf{M}_{c,k}$. $\mathbf{M}_{c,k}$ is a general BF matrix, that includes strategies such as zero forcing and stream wise power allocation. As scaling $\mathbf{M}_{c,k}$ by a scalar does not change the spanning property of $\mathbf{M}_{c,k}$, the BF matrix at the base station can be written as

$$\mathbf{Q}_{c,k} = \sqrt{\alpha_{c,k}} \cdot \mathbf{M}_{c,k} \qquad \alpha_{c,k} \in \mathbb{R},$$

where the BS transmit power intended for $\mathrm{RS}_k^{(c)}$ can easily be controlled by choosing $\alpha_{c,k}$ appropriately. The resulting transmit power at $\mathrm{BS}^{(c)}$

$$P_{\mathrm{BS}^{(c)}} = \sum_{k=1}^{N_\mathrm{R}} \mathrm{Tr}\left\{\mathbf{Q}_{c,k}\mathrm{E}\left[\mathbf{s}_{c,k}{\mathbf{s}_{c,k}}^H\right]{\mathbf{Q}_{c,k}}^H\right\} = \sum_{k=1}^{N_\mathrm{R}} \mathrm{Tr}\left\{\mathbf{Q}_{c,k}{\mathbf{Q}_{c,k}}^H\right\} = \sum_{k=1}^{N_\mathrm{R}} \alpha_{c,k} \cdot \mathrm{Tr}\left\{\mathbf{M}_{c,k}\mathbf{M}_{c,k}^H\right\}$$

is determined by adding up the transmit power in the individual sub channels that are directly proportional to the corresponding α.

How these parameters are influenced depends on the control objective. In the following sections, three different power control algorithms that go for different objectives and differently adapt power are presented.

4.2 Minimize Power

The optimization objective of the algorithms elaborated in this section is to achieve a certain target rate R_T by using minimal transmit power. First, different approaches are implemented and tested within a single cell. Then, simulation results in this simplified environment are evaluated and the best approaches are chosen to be extended to the whole carpet. After considering relay optimization and base station optimization separately, these two schemes can finally be combined to a joint optimization scheme that aims to minimize the transmit power under the given constraint on the rate.

In the first approaches presented in Section 4.2.1 to 4.2.3, the algorithm tries to enforce the target rate at all relays. Convergence problems of the algorithm and the problem of the power growing unboundedly ask for a more stable adapted algorithm. This improved algorithm allows to take some relays out of the network. It seems natural to take out the relay that achieves the lowest rate at the corresponding mobile. This empirical choice can be verified by considering indicators for the quality of the channel. However, the problem of unacceptable high power is still not completely eliminated. One idea of accessing this problem is to introduce an upperbound on the allowed transmit power, which can easily be implemented but eventually results again in convergence problems. The second approach presented in section 4.2.5 suggests a alternative solution that resolves the problem of unacceptable high power and at the same time guarantees convergence. More detailed descriptions of the two approaches and the different algorithms mentioned above are given in the following sections.

4.2.1 Enforce a Target Rate by Using Minimum Power

This algorithm defines a target rate R_T that is to be achieved for every mobile that belongs to one relay, irrespective of the needed transmit power.

The algorithm starts with equally distributed power at all relays within the cell of interest, denoted by c. Then, in turn, according to the numbering, for each relay the power is adjusted according to the actual rate at the corresponding mobile. The power update equation in the n^{th} iteration step

$$P_{\mathrm{RS}_i^{(c)}}^{(n+1)} = \frac{R_\mathrm{T}}{R_{c,i}^{(n)}} \cdot P_{\mathrm{RS}_i^{(c)}}^{(n)} \tag{4.2}$$

guarantees that the relay power is increased if the resulting rate is below the target rate and reduced if R is higher than R_T. As soon as the target rate is achieved, the power is not adapted anymore. After determining the new relay transmit power, the relay gain matrix $\mathbf{G}$ has to be adjusted in order to apply the change to the network.

$$\mathbf{G}_{c,i}^{(n+1)} = \beta_{c,i}^{(n+1)} \cdot \mathbf{I} = \sqrt{\frac{P_{\mathrm{RS}_i^{(c)}}^{(n+1)}}{\mathrm{Tr}\left\{\mathrm{E}\left[\mathbf{y}_{c,i}^{(\mathrm{R})} \mathbf{y}_{c,i}^{(\mathrm{R})^H}\right]\right\}}} \cdot \mathbf{I} \tag{4.3}$$

Then, for the new parameters the achievable rates at all mobiles

$$R_{c,k} = \log_2 \det\left(\mathbf{I} + \left(\mathbf{K}_\mathrm{n}^{(c,k)} + \mathbf{K}_\mathrm{i}^{(c,k)}\right)^{-1} \cdot \mathbf{K}_\mathrm{s}^{(c,k)}\right) \quad \forall k, \tag{4.4}$$

are determined, where the covariance matrices $\mathbf{K}_\mathrm{n}$, $\mathbf{K}_\mathrm{i}$ and $\mathbf{K}_\mathrm{s}$ are calculated according to (3.2) - (3.4)

The iteration over the relays is repeated as long as there is some rate that deviates from R_T by more than a given tolerance, ϵ, that is chosen to be $\epsilon = 10^{-2}$ for simulations.

As soon as convergence is achieved, the algorithm stops and outputs the momentaneous power distribution and the corresponding set of achievable rates, that all lie within a small interval around R_T.

Algorithm 1 summarizes the execution of the algorithm.

Algorithm 1 Power Minimization 1

1: Initialization: $P_{\mathrm{RS}_i^{(c)}} = 6\mathrm{W}\ \forall i$
2: Given: **Q**: ZF,WF
3: **while** some $\|R_i^{(c)} - R_\mathrm{T}\|_2 > \epsilon$ **do**
4: **for** $i = 1 : N_\mathrm{R}$ **do**
5: adjust $P_{\mathrm{RS}_i^{(c)}}$ accirding to (4.2)
6: adapt $G_{c,i}$ according to (4.3)
7: calculate $R_{c,i}\ \forall i$ according to (3.1)
8: **end for**
9: **end while**

In Figure 4.6, the convergence behavior of Algorithm 1 is illustrated. The curves in the first plot show how the rate for each mobile changes in each iteration and the second plot shows how power evolves, that leads to the upper rates. It can be seen that for this sample network constellation convergence is achieved within a few iterations and equal rate results at all mobiles. But one can also observe that the power allocated to RS_1 is approximately 150 W, which is not acceptable in practical networks.

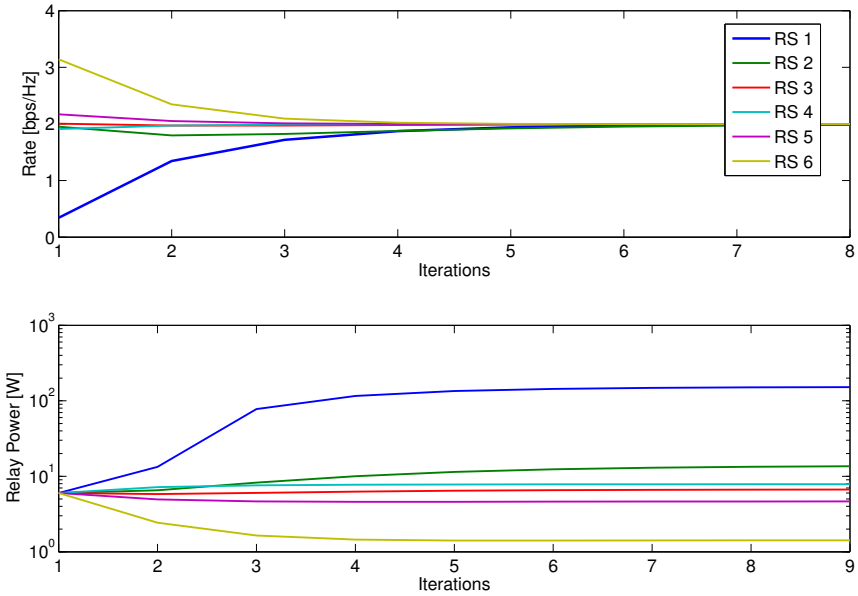

Figure 4.1: Rate and Power evolution at the individual relays, using $R_\mathrm{T} = 2$.

The possibly very high power required at some relays seems to be one problem of this algorithm. Further, by applying the algorithm to many different, randomly generated network constellations problems in convergence can also be observed. One example scenario where convergence is not achieved and interference problems lead to unbounded increase in power is shown in Figure 4.2. Therefore, the aim of simultaneously ensuring a target rate for each mobile turned out not to be achievable for certain network constellations. In case of a very bad channel coefficient between one relay and the corresponding mobile, the iterative increase of the transmit power in order to achieve the target rate results in increasing interference at the other nodes. This, again, enforces the latter to increase their own transmit power in order not to fall below the target rate and thereby again reduces the rate of the others. This kind of network constellations are called infeasible, as described in [17], and the algorithm does not converge, which leads to never ending iterative increase in power.

In order to prevent this undesired positive feedback scenario and to ensure convergence, in a second approach, the requirement of guaranteeing R_{T} at all mobiles is loosened to only ensure R_{T} at most of the mobiles.

4.2.2 Allowing Some Relays to be Turned Off

This approach aims to suppress the bad case scenarios of positive feedback and no convergence in case of an inconvenient network constellation.

First, the characteristic of the beamforming matrix $\mathbf{Q}$ of the base station is taken into account. As the base station is performing block zero forcing $\mathbf{Z}_{c,k}$ and does power loading with waterfilling $\mathbf{P}_{c,k}$, it is possible that some relay antennas do not get any power allocated due to their bad channel to the base station. In order to regard the initial situation of the relay nodes the target rate at each mobile is adapted to the initially available power at the relay. This is realized by choosing the target rate to be the number of active channels between the base station antennas and the corresponding relay.

$$R'^{(c)}_{\mathrm{T},k} = \#\text{ nonzero elements on the diagonal of } \mathbf{P}_{c,k}$$

By adapting the target rate, scenarios, where one relay is not supported by the base and nevertheless increases its transmit power, trying to achieve R_{T}, are avoided. If there are still convergence problems or some mobiles do not reach R'_{T} within an acceptable power range, despite the adapted target rate, the relay-mobile channel is account for the convergence problem. Situations where R_{T} can not be reached or power raises unacceptably high are identified and the algorithm is stopped. In this situation, either the actual power distribution and the resulting set of achievable rates are outputted, or one of the turn off strategies is applied.

Turn Off Strategies

It is assumed that relays whose signals achieve rates less than the target rate R_{T} are of little use. Therefore, three different turn off strategies that allow to turn off relays are developed in this section.

Turning off relays practically means that some mobiles are currently not served by the base station and not supported by the network. In this situation the user has to be scheduled to a different time or frequency resource block. This situation is in general undesirable. Nevertheless, if the date rate achieved at the mobile is negligible despite huge power, turning

off the relay and thereby eliminating interference at other users is reasonable in terms of power consumption,

turn off all In this approach, all nodes whose signal does not achieve the target rate are turned off. Thus, the interference caused by these nodes is eliminated and the remaining nodes can eventually reduce their transmit power without falling below R_{T}.

turn off worst A second approach is not to turn off all relays that do not reach the target rate, but only giving up on the one with the worst performance. This relay is identified by the highest actual power need, which also leads to the highest interference. Thereby, eventually less relays have to be turned off, as eliminating interference from one node my cause an other rate to be increased and thus achieving R_{T}. If there are still some rates that do not reach R_{T} after one relay is turned off, these strategy can be applied again until there is no rate at the remaining mobiles smaller than R_{T}

try all A third idea is to turn off all relays in turn and decide for the one that results in the highest benefit for the network.

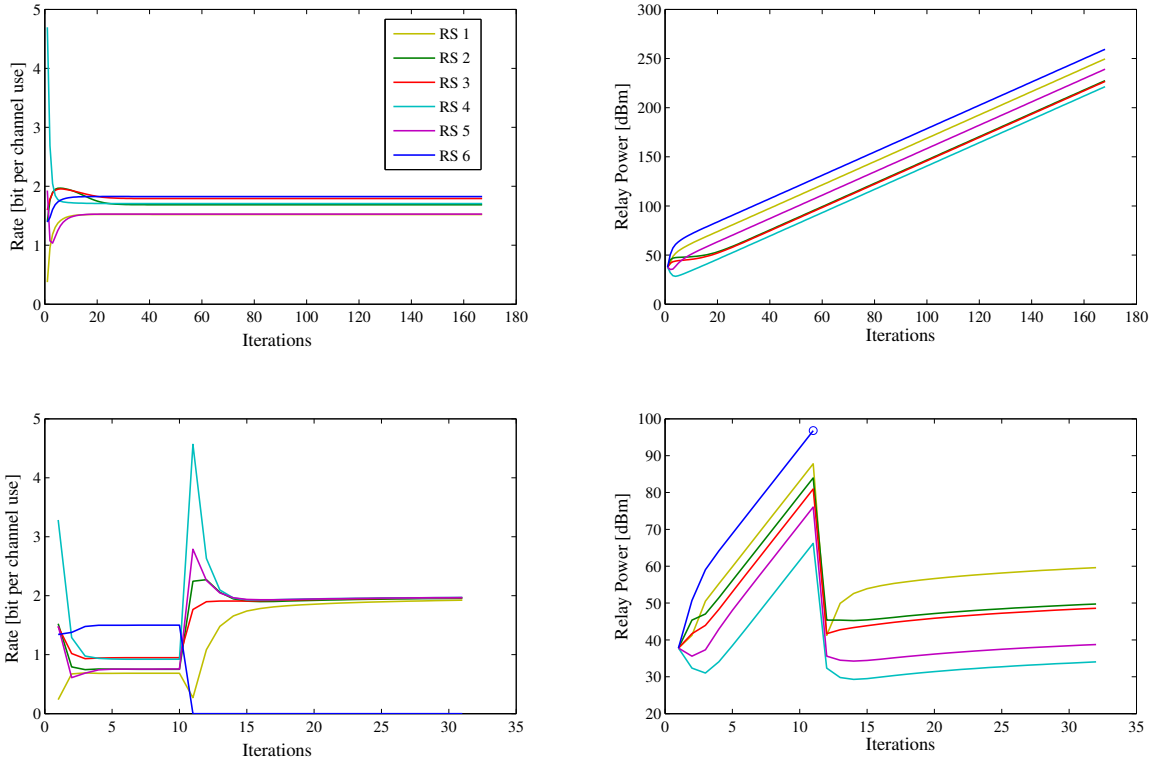

Figure 4.2: Effect of turning off one relay on the rate and power evolution, for no turn off (upper plots) and turn off worst (lower plots), $R_{\mathrm{T}} = 2$.

Figure 4.2 shows a sample scenario where the rate does not converge and the effect of turning off the relay with the worst performance. The upper plots show power and rate evolution of Algorithm 1 and the curves in the lower plots show the results of turning off one

relay. It can be observed that after 10 iterations a problem is detected and the relay with the highest power needed, RS_6, is turned off. This leads to an achievable rate of 0 bit per channel use at RS_6 and to an increase in rate at most of the other mobiles. Before turning off RS_6 none of the relays was able to achieve R_T but as interference from RS_6 is eliminated all the remaining relays reach R_T and convergence is achieved. Turning off all relays that do not reach R_T immediately would have been a bad choice in this case.

The turn off strategy in the example network of Figure 4.2 is applied as vanishing rate changes and monotonically increasing power indicate a convergence problem of Algorithm 1.

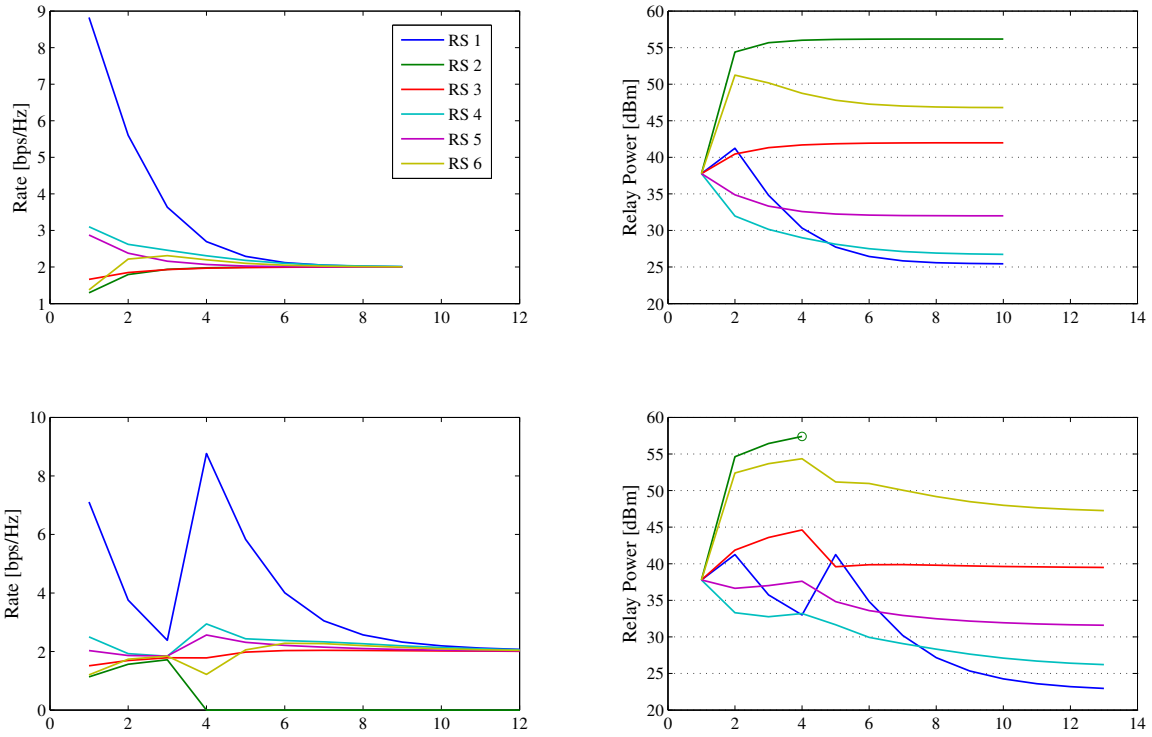

Figure 4.3: Effect of turning off one relay on the rate and power evolution, for no turn off (upper plots) and turn off worst (lower plots), $R_T = 2$ bps/Hz, P_{max}=200 W.

Figure 4.3 shows the second scenario where turn off strategies can be applied. In order to prevent too high powers in the network, relays are turned off if a predefined maximum power is exceeded.

In the lower plots it can be observed that, after 4 iterations, RS_2 is turned off, as it exceeds a maximum defined power of 200 W. This leads to an achievable rate of zero at MS_2 and an increase in rate at most of the other mobiles, as interference from RS_2 is eliminated. The resulting gap between the actual rate and R_T allows to further decrease transmit power. Thereby, further savings in power can be achieved. Transmit power at RS_1, RS_4, RS_5 and RS_6 is only slightly changed, but at RS_3 power can be decreased from 16 W to 9 W by turning off RS_1 that consumes 414 W.

The turn off strategies result in the expected gain and the large savings in power justify the penalty of reallocating the user to a different resource block.

4.2.3 Prediction

The idea of the prediction approach is to identify relays whose signal never reaches the target rate and take them out of the network in advance. The prediction is based on the analysis of the channel between relay station and mobile station. The singular values of the channel matrix $\mathbf{F}$ serve as a reliable indicator for the resulting performance in the achievable rate of the corresponding relay. As there are M_{M} singular values for each channel, we consider the sum of the squared singular values $\xi_{k,i}^{(c)}=\mathrm{Tr}\left\{\mathbf{F}_{k,i}^{(c,c)}\mathbf{F}_{k,i}^{(c,c)^H}\right\}$ as an indicator for the quality of the channel from relay i in cell c to mobile k in cell c. A reference value for mobile station $\mathrm{MS}_k^{(c)}$ is defined by

$$\lambda_k^{(c)} = \frac{\xi_{k,k}^{(c)}}{\sum_{j=1,j\neq k}^{N_{\mathrm{M}}} \xi_{k,j}^{(c)}},$$

where $\lambda_k^{(c)}$ can be interpreted as an approximation of the SIR at the receiver mobile $\mathrm{MS}_k^{(c)}$. As a second reference value serves

$$\gamma_k^{(c)} = \frac{\sum_{j=1,j\neq k}^{N_{\mathrm{M}}} \xi_{j,k}^{(c)}}{\xi_{k,k}^{(c)}},$$

this measures interference caused by $\mathrm{MS}_k^{(c)}$. If the ratio $\nu_k^{(c)} = \frac{\lambda_k^{(c)}}{\gamma_k^{(c)}}$ is smaller than a certain threshold, τ, a resulting turn off of the relay can mostly be predicted. The value of this threshold is empirically chosen to be $\tau = 1$. If there is some $\nu_k^{(c)}$ below τ, the relay $\mathrm{RS}_i^{(c)}$ with the lowest reference value is turned off and $\lambda_k^{(c)}$ and $\gamma_k^{(c)}$ are calculated again for the remaining nodes.

This is repeated as long as there is some value $\frac{\lambda_k^{(c)}}{\gamma_k^{(c)}} < \tau$.

k	RS_1	RS_2	RS_3	RS_4	RS_5	RS_6
$\lambda_k^{(c)}$	2.22	31.15	7.35	176.96	12.31	0.06
$\gamma_k^{(c)}$	11.94	0.97	0.10	0.002	0.02	1.31
$\frac{\lambda_k^{(c)}}{\gamma_k^{(c)}}$	0.19	32.10	71.04	72254	725	0.05

Table 4.1: Reference values for prediction

For the network constellation chosen in Figure 4.2, where we had no convergence, we get the reference values in table 4.1.

The turn off of RS_6 that results in convergence could have been predicted by considering these values.

4.2.4 Simulation Results

In Figure 4.4, the CDF of the individual rates at the mobiles and the CDF of the relay power in the cell of interest in dBm are shown. These curves arise from simulating the different power

control schemes for more than 1500 different network constellations. The green curve shows the results if no power control is applied and all relays have 6W transmit power available. The results of applying Algorithm 1 for $R_{\mathrm{T}} = 2$ are shown in red. The blue and the magenta curve arise from simulating two different turn off strategies, namely, 'try all 'and 'turn off worst'. A slight advantage of 'try all' over 'turn off worst' in terms of power consumption is visible. However, this small improvement in rate is in general not worth the large complexity needed to find the best relay. The yellow curves show the results for the prediction approach that aims to predict the blue curve. There are some deviations but over all the prediction is quite successful and the low complexity of the prediction approach is a big advantage.

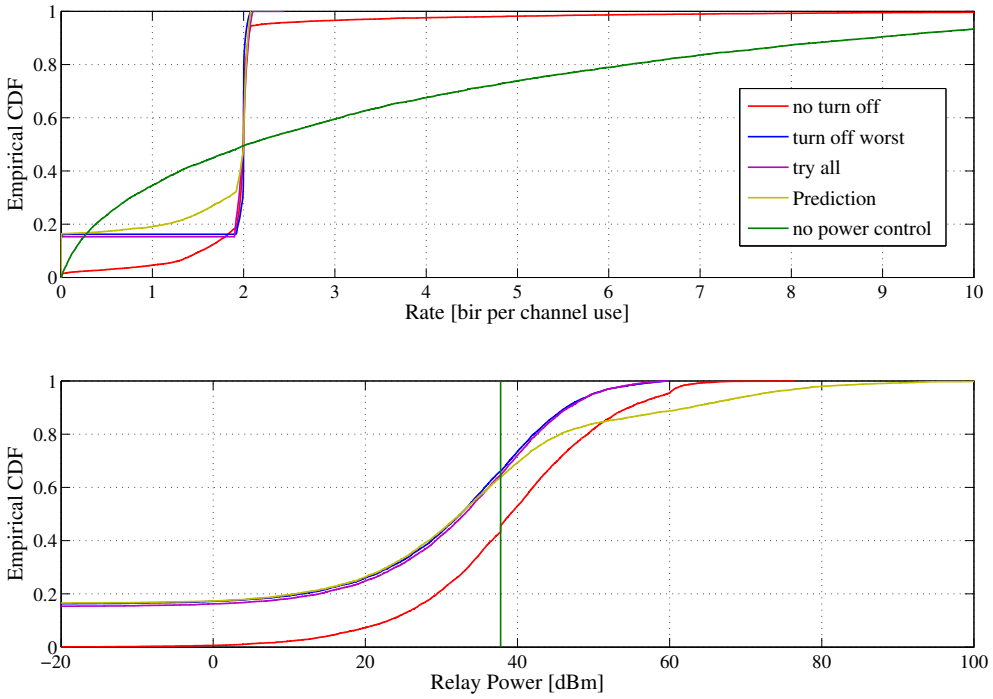

Figure 4.4: Empirical CDF of the individual rates and CDF of the relay power needed for different Minimize Power schemes.

4.2.5 2nd Approach: Power Minimization

In this section a different approach is developed, which limits the huge power consumption of the latter and nevertheless guarantees convergence. The main point is to define an initial maximal power allocation and only allow to lower transmit power. Thereby, the problem of unbounded increase of interference and power is eliminated and convergence can be guaranteed. Further, we assume the base station to perform zero forcing and the power to be equally distributed, which means that waterfilling at the base station is switched off.

Relay Optimization

In this section power control is only applied to the relays within a desired cell, c. Base station power control is discussed in Section 4.2.5

Initially, all relays have the same amount of given transmit power available. Starting from this given maximum power $P_{\mathrm{r,max}}$ at all relays, in each step the relay which achieves the highest rate at the corresponding mobile is indentified. Then, the power of this relay is reduced in the following way:

$$P_{\mathrm{RS}_l^{(c)}}^{(n+1)} = P_{\mathrm{RS}_l^{(c)}}^{(n)} - \mu \cdot P_{\mathrm{RS}_l^{(c)}}^{(n)} \left(1 - \frac{R_{\mathrm{T}}}{R_{c,l}}\right), \tag{4.5}$$

where μ is a stepsize parameter that is initially chosen to be 1 and can be adapted in case of oscillation problems. The update equation in (4.5) reduces the power based on the ratio of the desired and the actual rate. Again, we are guaranteed to have no change in rate as soon as the target rate is achieved.

The change in power is applied to the network by updating $\mathbf{G}$

$$\mathbf{G}_{c,i}^{(n+1)} = \beta_{c,i}^{(n+1)} \cdot \mathbf{I} = \sqrt{\frac{P_{\mathrm{RS}_i^{(c)}}^{(n+1)}}{\mathrm{Tr}\left\{\mathrm{E}\left[\mathbf{y}_{c,i}^{(\mathrm{R})} \mathbf{y}_{c,i}^{(\mathrm{R})H}\right]\right\}}} \cdot \mathbf{I} \tag{4.6}$$

and then the new set of achievable rates

$$R_{c,k} = \log_2 \det\left(\mathbf{I} + \left(\mathbf{K}_{\mathrm{n}}^{(c,k)} + \mathbf{K}_{\mathrm{i}}^{(c,k)}\right)^{-1} \cdot \mathbf{K}_{\mathrm{s}}^{(c,k)}\right), \quad \forall k, \tag{4.7}$$

is calculated using the updated parameters and equations (3.2) - (3.4).

These steps are repeated as long as there is some rate that exceeds the target rate R_{T} by more than some tolerance, that is chosen to be $\epsilon = 10^{-2}$ for simulations. If convergence is achieved, the current power distribution and the set of achievable rates is outputted.

Algorithm 2 summarizes the modified algorithm.

Algorithm 2 Power Minimization 2

1: Given: cell of interest, c
2: Initialization: $P_{\mathrm{RS}_i^{(c)}} = P_{\mathrm{r,max}}\ \forall i$
3: **while** some $R_{c,i} > R_{\mathrm{T}} + \epsilon$ **do**
4: find highest rate $R_{c,k}$
5: reduce $P_{\mathrm{RS}_k^{(c)}}$ according to (4.5)
6: adapt $G_{c,k}$ according to (4.6)
7: calculate $R_{c,i}\ \forall i$ according to (4.7)
8: **end while**

Base Station Optimization

Similar to the optimization of the relays in the last section, the transmit power at the base station can be controlled in order to achieve the required objective. Instead of adapting the

transmit power at the individual relays, the power allocated to each subchannel between BS and RS is controlled at the base station and the relay gain is kept constant.

Starting with equal distributed power and zero forcing at each BS, $\mathbf{Q}_{c,k} = \mathbf{Z}_{c,k}\ \forall k, c$, the BS power control algorithm proceeds in the same way as the relay optimization Algorithm 2. In every iteration, the highest rate $R_{c,k}$ in the selected cell c is identified and the power of the corresponding subchannel at the base station is reduced. The update is performed via the control parameter $\alpha_{c,k} \in [0, 1]$ according to equation (4.10) which is derived in the next section.

The power update is applied to the network by scaling the zero-forcing beamforming matrix by the new value of $\alpha_{c,k}$

$$\mathbf{Q}_{c,k}^{(n+1)} = \alpha_{c,k}^{(n+1)} \cdot \mathbf{Z}_{c,k}. \tag{4.8}$$

Using the updated parameters, the new set of achievable rates is determined according to (4.7).

These steps are repeated as long as there is some rate that exceeds the target rate by more than some tolerance, that is again chosen to be 0.01 for simulations. If convergence is achieved, the actual BS power distribution

$$P_{\mathrm{BS}_k^{(c)}} = \alpha_{c,k} \cdot \frac{P_{\mathrm{b,max}}}{N_{\mathrm{R}}} \tag{4.9}$$

and the resulting set of achievable rates are outputted.

Power Update Equation

In this section an update equation for the base station transmit power is proposed and motivated. The derivation shows an important property of the chosen update equation, that is of great importance for the performance and the convergence of the algorithm.

We propose:

$$\alpha_{c,k}^{(n+1)} = \alpha_{c,k}^{(n)} - \frac{R_{c,k} - R_{\mathrm{T}}}{m} \qquad \text{where } m = \frac{1}{\ln(2)} \cdot \mathrm{Tr}\left\{ (\mathbf{K}_{\mathrm{n}}^{(c,k)} + \mathbf{K}_{\mathrm{i}}^{(c,k)})^{-1} \mathbf{K}_{\mathrm{s}}^{(c,k)} \right\}. \tag{4.10}$$

This update equation guarantees that the resulting updated rate never falls below R_{T}, which ensures a continuous improvement in every step and is essential for convergence.

For the derivation of the proposed base station power update, we assume the relay transmit power P_{r} to be constant and the zero-forcing beamforming matrix at the base station to be normalized, such that

$$\sum_{i=1}^{N_{\mathrm{R}}} \mathrm{Tr}\left\{ \mathbf{Z}_{c,i} \mathbf{Z}_{c,i}^H \right\} = P_{\mathrm{b,max}}.$$

This leads to legitimated choices of $\alpha \in [0, 1]$ that result in $\mathbf{Q} = \alpha \cdot \mathbf{Z}$ and

$$\sum_{i=1}^{N_{\mathrm{R}}} \mathrm{Tr}\left\{ \mathbf{Q}_{c,i} \mathbf{Q}_{c,i}^H \right\} \leq P_{\mathrm{b,max}}.$$

For the achievable rate we get $\forall \alpha$

$$\begin{aligned} R_{c,k} &= \log_2 \left[\det \left(\mathbf{I} + (\mathbf{K}_{\mathrm{n}}^{(c,k)} + \mathbf{K}_{\mathrm{i}}^{(c,k)})^{-1} \alpha_{c,k} \mathbf{K}_{\mathrm{s}}^{(c,k)} \right) \right] \\ &= \log_2 \left[\det \left(\mathbf{K}_{\mathrm{n}}^{(c,k)} + \mathbf{K}_{\mathrm{i}}^{(c,k)} + \alpha_{c,k} \mathbf{K}_{\mathrm{s}}^{(c,k)} \right) \right] - \log_2 \left[\det \left(\mathbf{K}_{\mathrm{n}}^{(c,k)} + \mathbf{K}_{\mathrm{i}}^{(c,k)} \right) \right] \end{aligned}$$

where

$$\begin{aligned} K_{\mathrm{s}}^{(c,k)} &= \sum_{d=1}^{N_{\mathrm{B}}} \sum_{j=1}^{N_{\mathrm{R}}} \sum_{d'=1}^{N_{\mathrm{B}}} \sum_{j'=1}^{N_{\mathrm{M}}} \mathbf{F}_{k,j}^{(c,d)} \mathbf{G}_{d,j} \mathbf{H}_{j}^{(d,c)} \mathbf{Z}_{c,k} {\mathbf{Z}_{c,k}}^{H} {\mathbf{H}_{j'}^{(d',c)}}^{H} \mathbf{G}_{d',j'}^{H} {\mathbf{F}_{k,j'}^{(c,d')}}^{H} \\ K_{\mathrm{i}}^{(c,k)} &= \sum_{b=1}^{N_{\mathrm{B}}} \sum_{\substack{i=1 \\ i \neq k}}^{N_{\mathrm{R}}} \sum_{d=1}^{N_{\mathrm{B}}} \sum_{j=1}^{N_{\mathrm{R}}} \sum_{d'=1}^{N_{\mathrm{B}}} \sum_{j'=1}^{N_{\mathrm{R}}} \mathbf{F}_{k,i}^{(c,d)} \mathbf{G}_{d,j} \mathbf{H}_{j}^{(d,b)} \mathbf{Q}_{b,i} \mathbf{Q}_{b,i}^{H} {\mathbf{H}_{j'}^{(d',b)}}^{H} \mathbf{G}_{d,j'}^{H} {\mathbf{F}_{k,j'}^{(c,d')}}^{H} \\ K_{\mathrm{n}}^{(c,k)} &= \sum_{d=1}^{N_{\mathrm{B}}} \sum_{j=1}^{N_{\mathrm{R}}} \sum_{d'=1}^{N_{\mathrm{B}}} \sum_{j'=1}^{N_{\mathrm{R}}} \mathbf{F}_{k,j}^{(c,d)} \mathbf{G}_{d,j} \sigma_{\mathrm{n}}^2 \mathbf{G}_{d',j'}^{H} \mathbf{F}_{k,j'}^{(c,d')} + \sigma_{\mathrm{w}}^2 \mathbf{I}. \end{aligned}$$

Using $\partial \left(\ln(\det(\mathbf{X})) \right) = \mathrm{Tr} \left(\mathbf{X}^{-1} \partial \mathbf{X} \right)$, we can write the derivative of the rate with respect to $\alpha_{c,k}$ as

$$\frac{\partial R_{c,k}}{\partial \alpha_{c,k}} = \frac{1}{\ln(2)} \mathrm{Tr} \left[\left(\mathbf{K}_{\mathrm{n}}^{(c,k)} + \mathbf{K}_{\mathrm{i}}^{(c,k)} + \alpha_{c,k} \mathbf{K}_{\mathrm{s}}^{(c,k)} \right)^{-1} \mathbf{K}_{\mathrm{s}}^{(c,k)} \right].$$

We want to find $\alpha_{c,k} \in [0,1]$ that maximizes the derivative of the rate.
We use $\partial \mathrm{Tr}(\mathbf{X}^{-1}) = \mathrm{Tr}(\partial \mathbf{X}^{-1}) = \mathrm{Tr} \left(-\mathbf{X}^{-1} \partial \mathbf{X} \mathbf{X}^{-1} \right)$ and get

$$\frac{\partial^2 R_{c,k}}{\partial \alpha_{c,k}^2} = \frac{1}{\ln(2)} \cdot \mathrm{Tr} \left[-(\mathbf{K}_{\mathrm{n}}^{(c,k)} + \mathbf{K}_{\mathrm{i}}^{(c,k)} + \alpha_{c,k} \mathbf{K}_{\mathrm{s}}^{(c,k)})^{-1} \mathbf{K}_{\mathrm{s}}^{(c,k)} \left(\mathbf{K}_{\mathrm{n}}^{(c,k)} + \mathbf{K}_{\mathrm{i}}^{(c,k)} + \alpha_{c,k} \mathbf{K}_{\mathrm{s}}^{(c,k)} \right)^{-1} \mathbf{K}_{\mathrm{s}}^{(c,k)} \right].$$

$\frac{\partial^2 R_{c,k}}{\partial \alpha_{c,k}^2} \stackrel{!}{=} 0$ yields that the maximum slope is achieved at $\alpha_{c,k} = 0$. Thus, we get the following upperbound on the slope of $R_{c,k}$

$$\begin{aligned} m = \frac{\partial R_{c,k}}{\partial \alpha_{c,k}} &\leq \frac{1}{\ln(2)} \cdot \mathrm{Tr} \left[\left(\mathbf{K}_{\mathrm{n}}^{(c,k)} + \mathbf{K}_{\mathrm{i}}^{(c,k)} + \alpha_{c,k} \mathbf{K}_{\mathrm{s}}^{(c,k)} \right)^{-1} \mathbf{K}_{\mathrm{s}}^{(c,k)} \right] \Bigg|_{\alpha_{c,k}=0} \\ &= \frac{1}{\ln(2)} \mathrm{Tr} \left[\left(\mathbf{K}_{\mathrm{n}}^{(c,k)} + \mathbf{K}_{\mathrm{i}}^{(c,k)} \right)^{-1} \mathbf{K}_{\mathrm{s}}^{(c,k)} \right]. \end{aligned}$$

As the logarithm is a concave function of $\alpha_{c,k}$, the rate curve $R_{c,k}(\alpha_{c,k})$ can be upper-bounded by the straight line $t = m \cdot \alpha_{c,k}$.

Thus,

$$\frac{R_{c,k}(\alpha_{c,k}) - R_{\mathrm{T}}}{\alpha_{c,k} - \alpha_{c,k}^*} \leq m \quad \forall \alpha_{c,k} \in [0,1],$$

where $R_{c,k} \left(\alpha_{c,k}^* \right) = R_{\mathrm{T}}$ holds. This leads to the given update equation (4.10) and guarantees $\alpha_{c,k}^{(n+1)} \geq \alpha_{c,k}^*$.

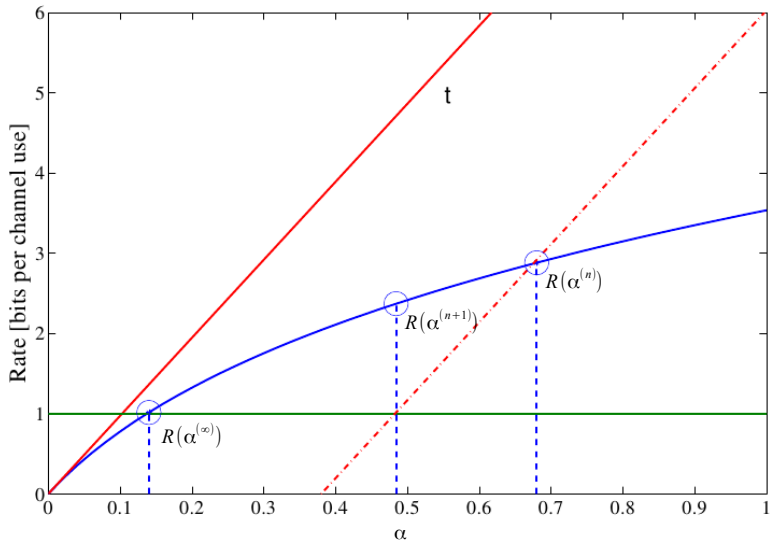

Figure 4.5: Geometric illustration of the base station power update.

In Figure 4.5 the upperbound is geometrically illustrated. The rate (blue) as a function of α is upperbounded by the straight line t (red). R_{T} is illustrated by the green line. The optimal value α^* is the value for which $R(\alpha^*) = R_{\mathrm{T}}$ and the α update is illustrated by the dashed lines. It is obvious that the updated rate always exceeds R_{T}.

Algorithm 3 summarizes the base station optimization algorithm explained.

Algorithm 3 BS Power Minimization

1: Given: cell of interest, c
2: Initialization: $\alpha_i = 1 \rightarrow P_{\mathrm{BS}_i^{(c)}} = \frac{P_{\mathrm{b,max}}}{N_{\mathrm{R}}}\ \forall i$
3: **while** some $R_{c,i} > R_{\mathrm{T}} + \epsilon$ **do**
4: find highest rate $R_{c,k}$
5: update $\alpha_{c,k}$ according to 4.10
6: adapt $Q_{c,k}$ according to 4.8
7: calculate $R_{c,i}\ \forall i$ according to 4.7
8: **end while**

4.2.6 Turn off Strategies

Turn off strategies can be applied to base station as well as to relay optimization. Similar to the relay power control scheme 4.2.2 we can derive turn off strategies for BS power control. Here, two schemes are implemented.

turn off all The first approach is to allocate zero power to the subchannels that do not fulfill the rate criteria after convergence of Algorithm 3. Then, provided that the power of the latter subchannels is set to zero, which means that this relay is taken out of the network, the optimizing Algorithm 3 is performed again and lower resulting transmit power is expected. This assumption is suitable as there is no interference caused by BSs that transmit at maximum power and nevertheless do not achieve the target rate.

turn off worst The second approach implemented is to allocate zero power only to one subchannel in each step and not giving up on all immediately. This subchannel is chosen to be the one with the highest power needed.

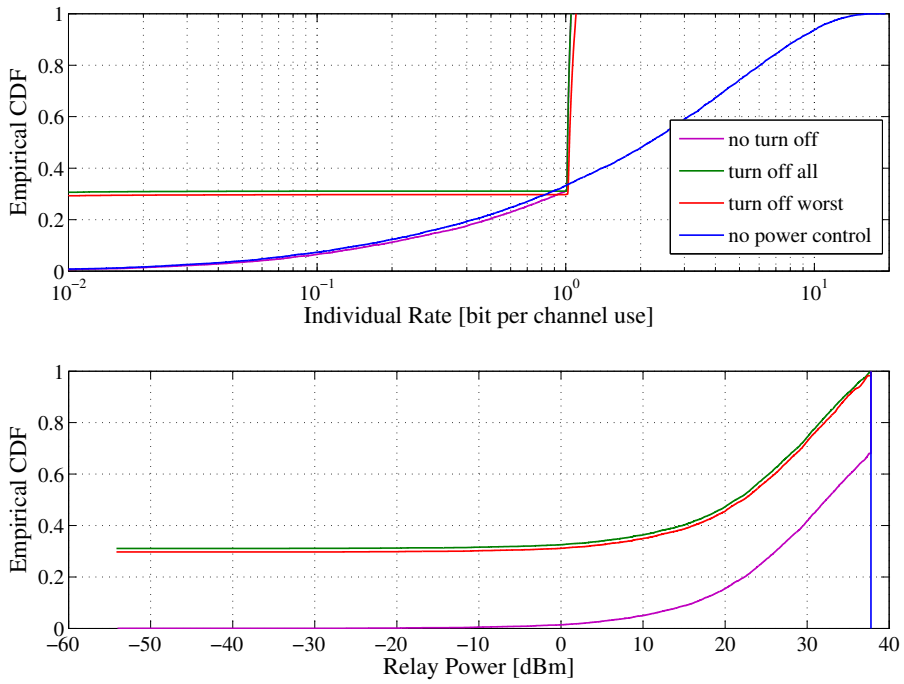

Figure 4.6: Rate and Power evolution at the individual relays for different turn off strategies, using $R_{\mathrm{T}} = 2$.

In Figure 4.6 the results of running Algorithm 2 and applying the two turn off strategies are shown. The first plot of Figure 4.6 shows the CDF of the individual achievable rates for the different turn off strategies and the second plot the CDF of the corresponding relay power in dBm.

	average Relay Power	av. N_{out}
no Power control	6 W	1.99
PC, no turn off	2.75 W	1.86
PC, turn off all	0.81 W	1.86
PC, turn off worst	0.90 W	1.77

Table 4.2: Numbers read from Figure 4.6

The blue curve shows the achievable rate of the Relay Carpet if no power control is applied and all relays transmit at a maximum power of 6 W. The results of applying relay power control according to Algorithm 2 are shown in magenta. Compared to the blue curve, there is a slight advantage in outage and a transmit power reduction of about 50 % by applying power control.

$$N_{\text{out}} = |\mathcal{L}^{(c)}| \text{ where } \mathcal{L}^{(c)} = \{l \in [1, ..., N_{\text{M}}] : R_{c,l} < R_{\text{T}}\}$$

Further, it can be observed, that turning off relays can save more than 60 % of power. As expected, a small improvement in rate and especially in outage can be achieved by successively taking relays out of the network (red) and not immediately giving up on all those whose signal does not achieve R_{T} (green). The power consumption of 'turn off worst' is slightly higher than the power consumption of 'turn off all' as there are less relays turned off.

4.2.7 Extension to the Whole Carpet

So far, we have only considered power control within one cell and the transmit power of the remaining carpet was assumed to be fixed during optimization. By including all cells to the optimization there are more parameters that can be influenced and further improvements are expected. The extension is performed by iterating over all cells starting in cell 1 and then proceeding according to the numbering of the cells. The extension can be applied to the relay optimization as well as to the base station optimization. Whereas for the derivation we only consider relay optimization.

Algorithm 4 starts by optimizing the power allocation in the first cell of the Relay Carpet using Algorithm 2. As soon as the optimization converges within the first cell, we continue by optimizing the second cell and proceed in the same manner until all N_{B} cells are optimized. After finishing the optimization in cell N_{B}, the rates in the first cell have increased, as there is less interference by transmit power reduction in the adjacent cells. This potential of optimization is used by iterating again over all cells starting at cell 1. The algorithm terminates if convergence is achieved considered over the whole carpet.

4.2.8 Joint Optimization

So far we have only considered relay and base station optimization separately. In this section, we are combining these two approaches to a joint optimization scheme running on the whole Relay Carpet.

There is one problem when considering joint optimization, which is the following: If we consider one cell and first optimize the relay power allocation within this cell, then, all mobiles already achieve R_{T} and lowering base station power can only have a non improving

Algorithm 4 RS Power Minimization extended

Initialization: $P_{\mathrm{RS}_i^{(c)}} = P_{\mathrm{r,max}}\ \forall c, i$
while some $R_{c,i} > R_{\mathrm{T}} + \epsilon$ **do**
  for $b = 1 : N_{\mathrm{B}}$ **do**
    run Alogrithm 2 starting from $P_{\mathrm{RS}_i^{(b)}}$
    update $P_{\mathrm{RS}_i^{(b)}}$
  end for
end while

effect. Therefore, iteratively running BS and RS optimization within one cell does not work. However, the extension to the whole carpet allows to solve this problem. Running the relay optimization Algorithm 2 once in each cell, offers a potential to optimize the base station power allocation in a second turn. Thereby, base stations and relays are optimized in turn as long as there is some mobile in the carpet that exceeds R_{T} by more than some tolerance, again chosen to be 0.01 for simulations.

Starting either by optimizing the BSs or the RSs results in slightly different results, shown in the next section.

Algorithm 5 summarizes the procedure of the algorithm starting by relay optimization.

Algorithm 5 Joint Optimization

Initialization: $P_{\mathrm{RS}_i^{(c)}} = P_{\mathrm{r,max}}\ \forall c, i$
while some $R_{c,i} > R_{\mathrm{T}} + \epsilon$ **do**
  for $b = 1 : N_{\mathrm{B}}$ **do**
    run Alogrithm 2 starting from $P_{\mathrm{RS}_i^{(b)}}$
    update $P_{\mathrm{RS}_i^{(b)}}$
  end for
  for $b = 1 : N_{\mathrm{B}}$ **do**
    run Alogrithm 3 starting from $P_{\mathrm{RS}_i^{(b)}}$
    update $P_{\mathrm{RS}_i^{(b)}}$
  end for
end while

4.2.9 Simulation Results

In this section, the different algorithms 2-5 are simulated in the Relay Carpet and the power allocation and the achievable rates are compared to the case where no power control is applied. 6 different schemes are simulated: No power control where the BS performs zero forcing and waterfilling (blue), relay optimization within one cell according to Algorithm 2 (green), relay optimization applied to the whole carpet, according to Algorithm 4 (magenta), base station power control extended to the whole carpet (yellow), joint optimization starting with relay optimization according to Algorithm 5 (black) and joint optimization starting with base station optimization (red).

In Figure 4.7, for all algorithms, results achieved in one cell, namely cell 1, are plotted in order to be able to compare results to Algorithm 2, for which cell 1 is chosen to be the desired cell. Some important numbers read from Figure 4.7 are summarized in Table 4.3

The first plot shows the CDF of the achievable rates at the mobiles. By comparing the outage, it can be observed, that the extended schemes perform all the same and slightly better than the optimization within one cell.

In the second plot the CDF of the transmit power at the relays is shown. The blue and the yellow schemes do not influence relay power and therefore the transmit power is equal to 6 W at every relay. By comparing the green to the magenta curve, a relay transmit power reduction of more than 10 % within cell 1 can be observed, which shows the benefit of the extension to the whole carpet.

The third plot shows the CDF of the transmit power at the base station. Again, we have three schemes that do not perform BS power control and therefore the base station transmits at maximum power, 40 W.

Overall, it can be seen that BS power control can lead to slightly higher savings in power than RS power control. Therefore, BSRS which starts by optimizing the BS outperforms RSBS that has only little potential to do BS optimization in the second turn.

	av. N_{out}	av. RS power	av. BS power	av. power per cell
no PC	2.01	6 W	40 W	76 W
RS one cell	1.87	2.74 W	40 W	56.44 W
RS extended	1.60	2.43 W	40 W	54.58 W
BS extended	1.60	6W	16.56 W	52.56 W
RSBS	1.60	2.70 W	33.29 W	49.49 W
BSRS	1.60	4.57 W	18.45 W	45.87 W

Table 4.3: Numbers read from Figure 4.7

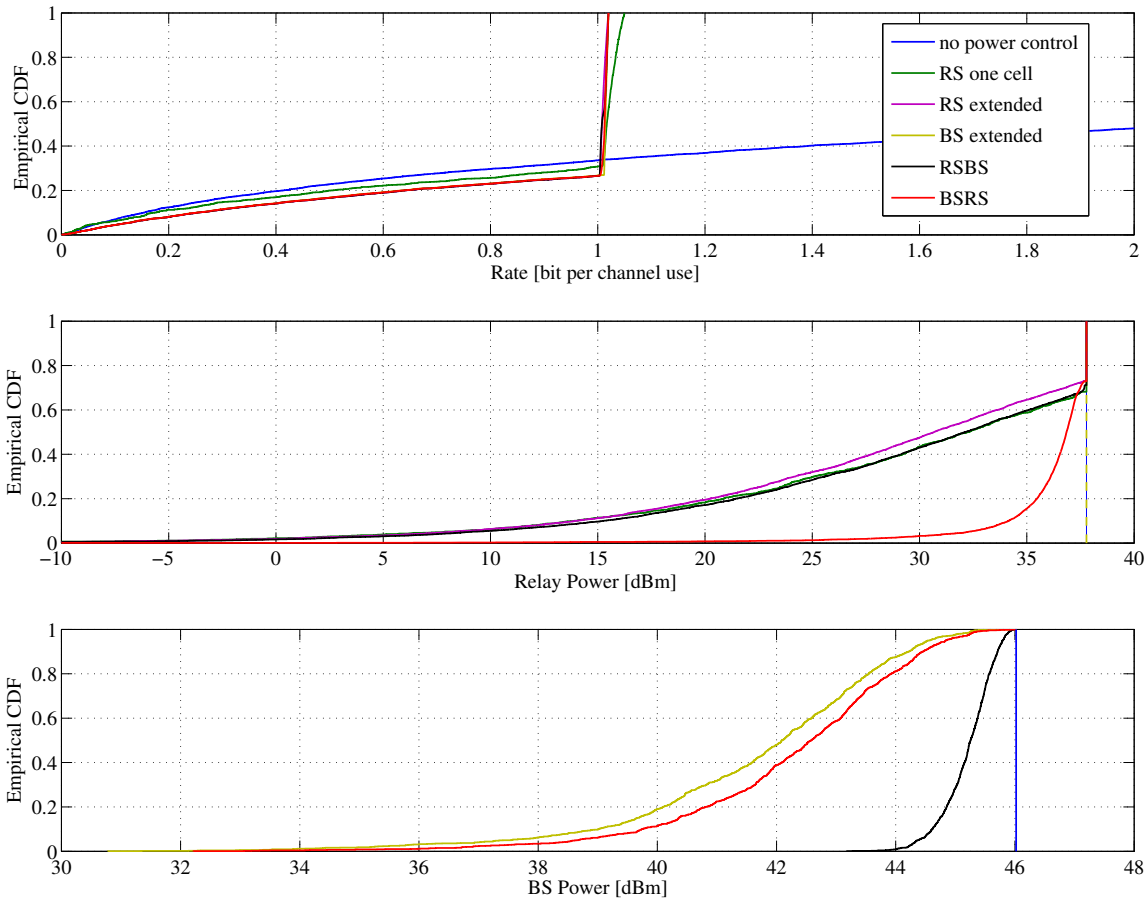

Figure 4.7: Comparison of the different schemes for power minimization for R_{T}=1 bit per channel use.

4.3 Maximize Minimum Rate

In this section, a different optimization objective, which is the maximization of the smallest rate at the receiver for a given transmit power, is considered and two different algorithms are elaborated. The base station performs zero-forcing and the BS sum transmit power is kept constant and distributed on the different links such that the power allocation can not be changed without resulting in a smaller minimum rate.

The algorithm converges as soon as the power is distributed in a way that results in equal rate, denoted by R_{conv}, at all relays. Hence, there is no link whose power can be reduced in favor of an other link, without reducing the minimum achievable rate.

First, a heuristic algorithm, that only operates within one cell is considered and then a gradient base algorithm that can be extended to the whole carpet is presented.

4.3.1 MaxMin Algorithm

The MaxMin algorithm presented in this section iteratively maximizes the minimum rate within a desired cell in a heuristic manner. For the derivation of the algorithm, we only consider base station power control, whereas a slightly modified algorithm can also be applied to the relays. Initially, power is equally distributed at the base station. Then, for the desired cell, in each step, the mobile $\mathrm{MS}_k^{(c)}$ that achieves the lowest rate $R_{\min}$ and the mobile $\mathrm{MS}_i^{(c)}$ that reaches the highest rate are determined. Then, the power at the base station allocated to $\mathrm{MS}_i^{(c)}$ is reduced by updating $\alpha_{c,i}$ similarly to (4.10):

$$\alpha_{c,i}^{(n+1)} = \alpha_{c,i}^{(n)} - \frac{R_{c,i} - R_{\min}}{m}, \tag{4.11}$$

which guarantees $R_{\min}^{(n+1)} \geq R_{\min}^{(n)}$ and leads to the updated BS power

$$P_{\mathrm{BS}_i^{(c)}}^{(n+1)} = \alpha_{c,i}^{(n+1)} \cdot \frac{P_{\mathrm{b,max}}}{N_{\mathrm{R}}}. \tag{4.12}$$

Then the saving in power $\Delta P = P_{\mathrm{BS}_i^{(c)}}^{(n)} - P_{\mathrm{BS}_i^{(c)}}^{(n+1)}$ is given to $\mathrm{MS}_k^{(c)}$, which leads to

$$\alpha_{c,k}^{(n+1)} = \left(P_{\mathrm{BS}_k^{(c)}}^{(n)} + \Delta P \right) \cdot \frac{N_{\mathrm{R}}}{P_{\mathrm{b,max}}}. \tag{4.13}$$

The power updates are applied to the network by updating the beamforming matrices

$$\mathbf{Q}_{c,j}^{(n+1)} = \sqrt{\alpha_{c,j}^{(n+1)}} \cdot \mathbf{Z}_{c,j}, \quad j \in \{i,k\} \tag{4.14}$$

Then, the set of achievable rates $R_{c,k}$, $\forall k$, using the new parameters is calculated. These steps are repeated as long as the highest and the lowest achievable rate within c differ by more than some tolerance, chosen to be $\epsilon = 10^{-2}$ for simulations. As soon as convergence is achieved, the current power distribution and the resulting set of achievable rates, that all lie within an small tolerance around R_{conv}, are outputted.

Algorithm 6 MaxMin

1: Given: desired cell, c
2: Initialization: $P_{\mathrm{BS}_i^{(c)}} = \frac{P_{\mathrm{b,max}}}{N_{\mathrm{R}}}$ $\forall c, i$
3: **while** $\left(\max_i(R_{c,i}) - \min_i(R_{c,i}) \right) > \epsilon$ **do**
4: find highest rate $R_{c,i}$
5: find $\mathrm{MS}_k^{(c)}$ with lowest rate $\mathrm{R}_{\min}$
6: update $\alpha_{c,i}$ according to (4.11)
7: update $\alpha_{c,k}$ according to (4.13)
8: update $\mathbf{Q}_{c,k}$ and $\mathbf{Q}_{c,i}$ according to (4.14)
9: calculate $R_{c,j}$ $\forall j$ according to (3.1)
10: **end while**

Algorithm 6 described in this section is a heuristic approach that can be applied to optimize power within one cell. However, an extension of this algorithm to the whole carpet is not

possible, as the achievable rate R_{conv} after convergence within one cell could be worsened by optimizing a second cell. Therefore, we consider a gradient based algorithm that solves the same optimization problem and can be extended to the whole carpet.

4.3.2 Gradient Search

The MaxMin optimization problem considered can be formulated as a maximization problem subject to a sum power constraint.

$$\begin{aligned} \underset{\alpha}{\text{maximize}} \quad & \min_i \{R_{c,i}(\alpha)\} \\ \text{subject to:} \quad & \sum_{k=1}^{N_\text{R}} P_{\text{BS}_k^{(c)}} = P_{\text{b,sum}}, \ \ \forall c. \end{aligned}$$

We consider a gradient based algorithm to find the optimal power allocation, α, over the whole carpet under the given sum power constraint. In the implementation of the gradient search algorithm the following approximation for the cost function is used:

$$R_{\text{min}}^{(c)} = \min_i \{R_{c,i}\} = \|[R_{c,1}, ..., R_{c,N_\text{R}}]\|_{-\infty} \approx \|[R_{c,1}, ..., R_{c,N_\text{R}}]\|_p, \ \ p \ll -1.$$

Further, the problem can be reformulated as an unconstrained optimization problem by substituting

$$\alpha_{c,i} = \frac{\widetilde{\alpha}_{c,i} \cdot P_{\text{b,sum}}}{\sum_{i=1}^{N_\text{R}} \widetilde{\alpha}_{c,i}},$$

which changes the optimization variable to $\widetilde{\alpha}_{c,i}$ and guarantees to fulfill the sum power constraint. By scaling $\mathbf{Z}$ such that $\text{Tr}\left\{\mathbf{Z}_{c,k}\mathbf{Z}_{c,k}^H\right\} = 1 \ \forall c, k$, we can verify:

$$\sum_{k=1}^{N_\text{R}} P_{\text{BS}_k^{(c)}} = \sum_{k=1}^{N_\text{R}} \alpha_{c,k} \cdot \text{Tr}\left\{\mathbf{Z}_{c,k}\mathbf{Z}_{c,k}^H\right\} = \sum_{k=1}^{N_\text{R}} \alpha_{c,k} = \sum_{k=1}^{N_\text{R}} \frac{\widetilde{\alpha}_{c,k} \cdot P_{\text{b,sum}}}{\sum_{i=1}^{N_\text{R}} \widetilde{\alpha}_c, i} = P_{\text{b,sum}}.$$

We obtain the gradient vector of the cost function R_{min} by taking the derivative with respect to $\widetilde{\alpha}$

$$\nabla_{\widetilde{\alpha}} R_{\text{min}}^{(c)} = \begin{bmatrix} \frac{\partial R_{\text{min}}^{(c)}}{\partial \widetilde{\alpha}_{1,1}} \\ \cdot \\ \cdot \\ \frac{\partial R_{min}^{(c)}}{\partial \widetilde{\alpha}_{N_\text{B},N_\text{R}}} \end{bmatrix} = \nabla_\alpha R_{\text{min}}^{(c)\ T} \cdot \begin{bmatrix} \frac{\partial \alpha_{1,1}}{\partial \widetilde{\alpha}_{1,1}} & \frac{\partial \alpha_{1,1}}{\partial \widetilde{\alpha}_{1,2}} & \cdots & \frac{\partial \alpha_{1,1}}{\partial \widetilde{\alpha}_{N_\text{B},N_\text{R}}} \\ \cdots & \cdots & & \cdots \\ \frac{\partial \alpha_{N_\text{B},N_\text{R}}}{\partial \widetilde{\alpha}_{1,1}} & \frac{\partial \alpha_{N_\text{B},N_\text{R}}}{\partial \widetilde{\alpha}_{1,2}} & \cdots & \frac{\partial \alpha_{N_\text{B},N_\text{R}}}{\partial \widetilde{\alpha}_{N_\text{B},N_\text{R}}} \end{bmatrix} \tag{4.15}$$

where the entries of the Jacobian are:

$$\frac{\partial \alpha_{c,k}}{\partial \widetilde{\alpha}_{d,j}} = \begin{cases} 0 & \text{if } c \neq d \\ -\frac{P_{\text{b,sum}} \cdot \widetilde{\alpha}_{c,k}}{\left(\sum_i \widetilde{\alpha}_{c,i}\right)^2} & \text{if } c = d, k \neq j \\ \frac{P_{\text{b,sum}} \cdot \sum_{i,i\neq k} \widetilde{\alpha}_{c,i}}{\left(\sum_i \widetilde{\alpha}_{c,i}\right)^2} & \text{if } c = d, k = j. \end{cases}$$

Using the p-norm approximation, $R_{\min}^{(c)} = \left\| R^{(c)} \right\|_p$, the entries of the unconstraint gradient vector $\nabla_\alpha R_{\min}^{(c)}$

$$\frac{\partial R_{\min}^{(c)}}{\partial \alpha_{d,k}} = \frac{1}{p} \left({R_{c,1}}^p + {R_{c,2}}^p + ... + {R_{c,N_\mathrm{M}}}^p \right)^{\frac{1}{p}-1} \cdot \left(p \cdot {R_{c,1}}^{p-1} \frac{\partial R_{c,1}}{\partial \alpha_{d,k}} + ... + p \cdot {R_{c,N_\mathrm{M}}}^{p-1} \frac{\partial R_{c,N_\mathrm{M}}}{\partial \alpha_{d,k}} \right)$$

can be written as a function of the derivatives of the individual rates

$$\begin{aligned} \frac{\partial R_{c,i}}{\partial \alpha_{d,k}} &= \frac{\partial}{\partial \alpha_{d,k}} \log_2 \det \left[\mathbf{I} + \left(\mathbf{K}_{\mathrm{n+i}}^{(c,i)} \right)^{-1} \mathbf{K}_{\mathrm{s}}^{(c,i)} \right] \\ &= \frac{1}{\ln(2)} \mathrm{Tr} \left\{ \left(\mathbf{K}_{\mathrm{n+i}}^{(c,i)} + \mathbf{K}_{\mathrm{s}}^{(c,i)} \right)^{-1} \left(\frac{\partial \mathbf{K}_{\mathrm{n+i}}^{(c,i)}}{\partial \alpha_{d,k}} + \frac{\partial \mathbf{K}_{\mathrm{s}}^{(c,i)}}{\partial \alpha_{d,k}} \right) \right\} - \frac{1}{\ln(2)} \mathrm{Tr} \left\{ \left(\mathbf{K}_{\mathrm{n+i}}^{(c,i)} \right)^{-1} \frac{\partial \mathbf{K}_{\mathrm{n+i}}^{(c,i)}}{\partial \alpha_{d,k}} \right\}. \end{aligned}$$

It remains to give closed expressions for $\frac{\partial \mathbf{K}_{\mathrm{s}}^{(c,i)}}{\partial \alpha_{d,k}}$ and $\frac{\partial \mathbf{K}_{\mathrm{n+i}}^{(c,i)}}{\partial \alpha_{d,k}}$. To this end, different cases are distinguished:

<u>case 1</u>: $c = d$, $i = k$

$$\begin{aligned} \frac{\partial \mathbf{K}_{\mathrm{s}}^{(c,i)}}{\partial \alpha_{d,k}} &= \sum_{b=1}^{N_\mathrm{B}} \sum_{j=1}^{N_\mathrm{R}} \sum_{b'=1}^{N_\mathrm{B}} \sum_{j'=1}^{N_\mathrm{M}} \mathbf{F}_{i,j}^{(c,b)} \mathbf{G}_{b,j} \mathbf{H}_j^{(b,c)} \mathbf{Z}_{c,i} {\mathbf{Z}_{c,i}}^H {\mathbf{H}_{j'}^{(b',c)}}^H \mathbf{G}_{b',j'}^H {\mathbf{F}_{i,j'}^{(c,b')}}^H \\ \frac{\partial \mathbf{K}_{\mathrm{n+i}}^{(c,i)}}{\partial \alpha_{d,k}} &= 0 \end{aligned}$$

<u>case 2</u>: $c = d$, $i \neq k$

$$\begin{aligned} \frac{\partial \mathbf{K}_{\mathrm{s}}^{(c,i)}}{\partial \alpha_{d,k}} &= 0 \\ \frac{\partial \mathbf{K}_{\mathrm{n+i}}^{(c,i)}}{\partial \alpha_{d,k}} &= \sum_{\substack{k=1 \\ k \neq i}}^{N_\mathrm{R}} \sum_{b=1}^{N_\mathrm{B}} \sum_{j=1}^{N_\mathrm{R}} \sum_{b'=1}^{N_\mathrm{B}} \sum_{j'=1}^{N_\mathrm{R}} \mathbf{F}_{i,j}^{(c,b)} \mathbf{G}_{b,j} \mathbf{H}_j^{(b,c)} \mathbf{Z}_{c,k} \mathbf{Z}_{c,k}^H {\mathbf{H}_{j'}^{(b',c)}}^H \mathbf{G}_{b',j'}^H {\mathbf{F}_{i,j'}^{(c,b')}}^H \end{aligned}$$

<u>case 3</u>: $c \neq d$

$$\begin{aligned} \frac{\partial \mathbf{K}_{\mathrm{s}}^{(c,i)}}{\partial \alpha_{d,k}} &= 0 \\ \frac{\partial \mathbf{K}_{\mathrm{n+i}}^{(c,i)}}{\partial \alpha_{d,k}} &= \sum_{\substack{e=1 \\ e \neq c}}^{N_\mathrm{B}} \sum_{l=1}^{N_\mathrm{R}} \sum_{b=1}^{N_\mathrm{B}} \sum_{j=1}^{N_\mathrm{R}} \sum_{b'=1}^{N_\mathrm{B}} \sum_{j'=1}^{N_\mathrm{R}} \mathbf{F}_{i,j}^{(c,b)} \mathbf{G}_{b,j} \mathbf{H}_j^{(b,e)} \mathbf{Z}_{e,l} \mathbf{Z}_{e,l}^H {\mathbf{H}_{j'}^{(b',e)}}^H \mathbf{G}_{b',j'}^H {\mathbf{F}_{i,j'}^{(c,b')}}^H \end{aligned}$$

By putting eyerything together, we can compute the gradient of our cost function $\nabla_{\tilde{\alpha}} R_{\min}^{(c)}$ according to (4.15). A gradient search for the optimum power allocation α uses the update equation

$$\widetilde{\alpha}^{(n+1)} = \widetilde{\alpha}^{(n)} + \nabla_{\widetilde{\alpha}^{(n)}} R_{\min}^{(c)} \cdot \frac{\mu}{\left\| \nabla_{\widetilde{\alpha}^{(n)}} R_{\min}^{(c)} \right\|},$$

where μ is the stepsize parameter, which is chosen to be small enough to avoid large oszillations and to guarantee $\alpha \in [0, 1]$.

In Figure 4.8, the convergence behavior of the gradient search algorithm is shown. The first plot shows how the achievable rates at the mobiles within cell c evolve and the second plot shows how the cost function $\|R\|_p$ changes in each iteration. The stepsize is chosen to be 0.05 and reduced after 500 iterations, this can be seen in Figure 4.8 as oscillations are stopped at this point in time. The gradient search algorithm could be improved by implementing line search to find the optimum step size parameter in each step and thereby avoid the oszillations. However, this feature further increases complexity of the algorithm and is not treated in this thesis. In the second plot of Figure 4.8 the quality of the norm approximation is illustrated by plotting the actual minimum rate in red. The deviation of the red curve from the blue one is insignificant and justifies our approximation.

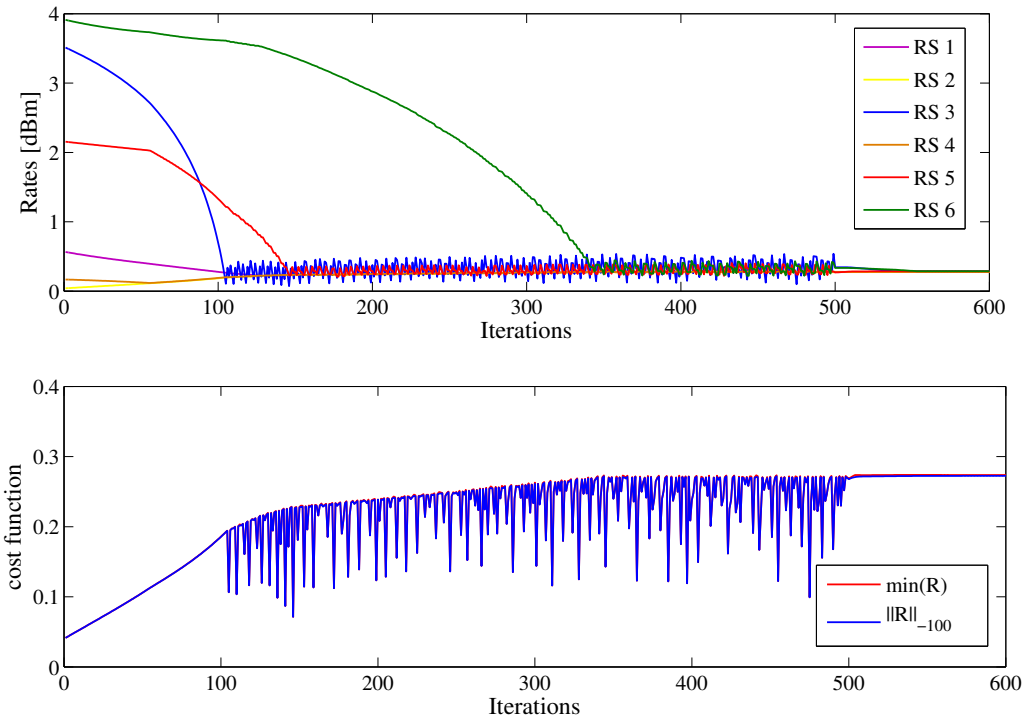

Figure 4.8: Illustration of the convergence of the gradient search algorithm. The evolution of the rates (upper plot) and the cost function (lower plot) are shown.

As we have derived the extended gradient search algorithm we can now simulate it for different network constellations and compare it to Algorithm 6. In the next section, the two algorithms are discussed based on simulation results.

4.3.3 Simulation Results

The heuristic MaxMin algorithm and the gradient based algorithm are simulated for different network constellations. The gradient search algorithm is simulated for the whole carpet as well as within a single cell. Figure 4.9 shows the CDF of the minimum rate per cell for the three different algorithms and the case where no power control is applied. The results achieved by the heuristic algorithm are nearly equivalent to the results achieved by running the gradient based algorithm within one cell. This is expected as they go for the same objective and have the same parameters available for optimization. But, the computational complexity of the gradient search algorithm is by orders of magnitude higher than of the heuristic algorithm and therefore a huge drawback. This complexity grows again by extending the scheme to the whole carpet. The MaxMin algorithm arrives to raise the smallest rate from 0.33 to 0.91 bit per channel use on average. A further improvement to an average smallest rate of 0.99 is achieved by the extension to the whole carpet. This improvement is achieved as the extension allows to control all base stations in the network and thereby all BSs can contribute to maximize the smallest rate within the desired cell.

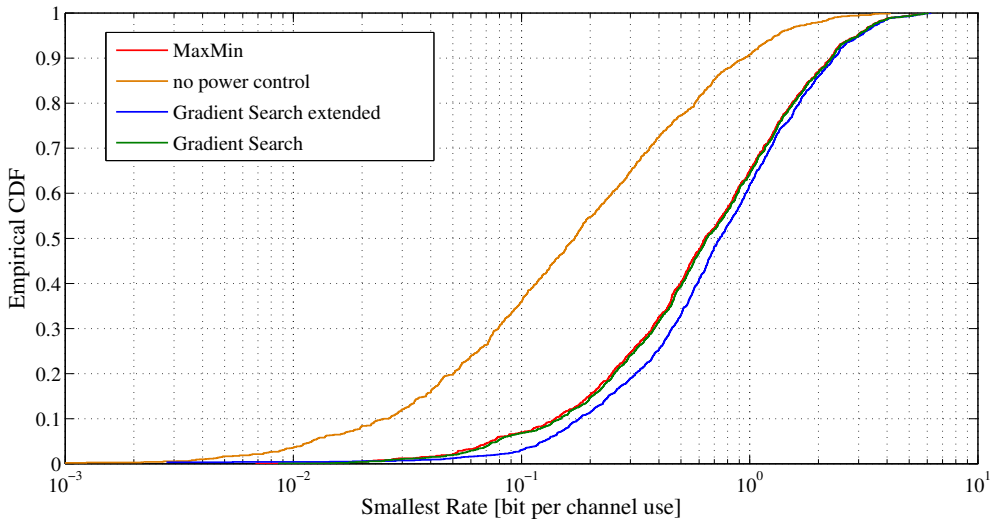

Figure 4.9: Illustration of the minimum rate per cell for the heuristic MaxMin algorithm (red), the gradient search algorithm within one cell (green) and the extended gradient search algorithm (blue) applied to the whole carpet.

4.4 Minimize Outage

In this section, algorithms are presented that aim to minimize the outage for a given available power at the BS. In contrast to the MaxMin algorithm that minimizes the outage from the point of view of the BS, that defines the outage as $\mathrm{I}(\exists i : R_{c,i} < R_{\mathrm{T}})$, we are now considering the outage of the individual users. We define

$$N_{\mathrm{out}} = |\mathcal{L}|, \text{ where } \mathcal{L} = \{l \in \{1...N_{\mathrm{M}}\} : R_{c,l} < R_{\mathrm{T}}\}$$

that is to be minimized. Therefore, for a certain target rate R_{T}, the transmit power for those MS that exceed R_{T} is reduced and allocated to the MS that is closest to reaching R_{T} such that the BS sum transmit power is kept constant. The algorithm converges as soon as there is no rate exceeding R_{T} by more than some tolerance ϵ.

The procedure of the algorithm is similar to Algorithm 6, only the power update is performed differently. Initially, there is $P_{\mathrm{b,max}}$ power available at each BS, then, for the desired cell, in each step, the mobile $\mathrm{MS}_i^{(c)}$ reaching the highest rate is identified. The power at $\mathrm{MS}_i^{(c)}$ is reduced by choosing

$$\alpha_{c,i}^{(n+1)} = \alpha_{c,i}^{(n)} - \frac{R_{c,i} - R_{\mathrm{T}}}{m}. \tag{4.16}$$

This guarantees $R_{c,i}^{(n+1)} > R_{\mathrm{T}}$ which is important to not get an additional outage. Then, the saving in power $\Delta P = P_{c,i}^{(n)} - P_{c,i}^{(n+1)}$ is given to $\mathrm{MS}_k^{(c)}$ with

$$k = \underset{l \in \mathcal{L}}{\operatorname{argmin}}\ R_{\mathrm{T}} - R_{c,l}.$$

This leads to

$$\alpha_{c,k}^{(n+1)} = \left(P_{c,k}^{(n)} + \Delta P\right) \cdot \frac{N_{\mathrm{R}}}{P_{\mathrm{b,max}}}. \tag{4.17}$$

The new power distribution is captured by adapting the beamforming matrix $\mathbf{Q}_{c,i}$ and $\mathbf{Q}_{c,k}$ as in (4.14). The new set of achievable rates is determined and then, these steps are repeated as long as there exists an l such that $R_{c,l} > R_{\mathrm{T}} + \epsilon$. After convergence, the current values for α and the corresponding set of achievable rates is outputted.

Algorithm 7 Minimize Outage

1: Given: cell of interest, c
2: Initialization: $\alpha_i = 1 \rightarrow P_{\mathrm{BS}_i^{(c)}} = \frac{P_{\mathrm{b,max}}}{N_{\mathrm{R}}}\ \forall i$
3: **while** $\exists l : R_{c,l} > R_{\mathrm{T}} + \epsilon$ **do**
4: find highest rate $R_{c,i}$
5: update $\alpha_{c,i}$ according to (4.16)
6: find $\mathrm{MS}_k^{(c)}$ with rate closest to R_{T}
7: update $\alpha_{c,k}$ according to (4.17)
8: adapt $Q_{c,k}$ according to (4.14)
9: calculate $R_{c,j}\ \forall j$ according to (4.7)
10: **end while**

4.4.1 Simulation Results

Figure 4.10 and 4.11 show simulation results obtained by applying Algorithm 7 to 1500 different network constellations. The first plot of Figure 4.10 shows the CDF of the achievable rates at the mobiles and the second plot illustrates the outage per cell, N_{out}. The results from Algorithm 7 (red) are compared to the values achieved in the Relay Carpet without applying power control (blue). A significant improvement in outage per cell from 2.23 to 1.29 on average can be achieved by applying power control.

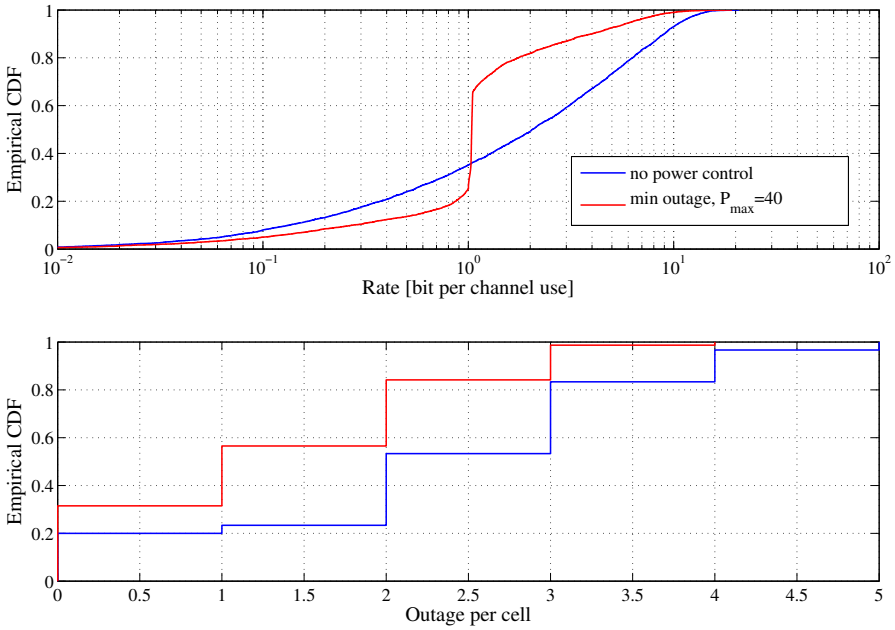

Figure 4.10: Comparison of achievable rates and outage for Minimize Outage and no power control.

Figure 4.11 shows the results of running Algorithm 7 for different values of $P_{\text{b,max}}$. It can be observed, that reducing transmit power at the BS from 40 W to 20 W results in a larger number of cells having an outage of 2 and higher. This comes from the lower transmit power available at the base station that achieve R_{T}. If there are just few BS whose power can be reduced and this power is small, the chance to arrive at raising the rate at another mobile higher than R_{T} is small, even if they are close to R_{T}. However, depending on the application, the savings in power can be more important than the slight drop in performance.

$P_{\text{b,max}}$	40	20	10	5	1
av. N_{out}	1.29	1.53	1.56	1.60	1.98

Table 4.4: Numbers read from Figure 4.11

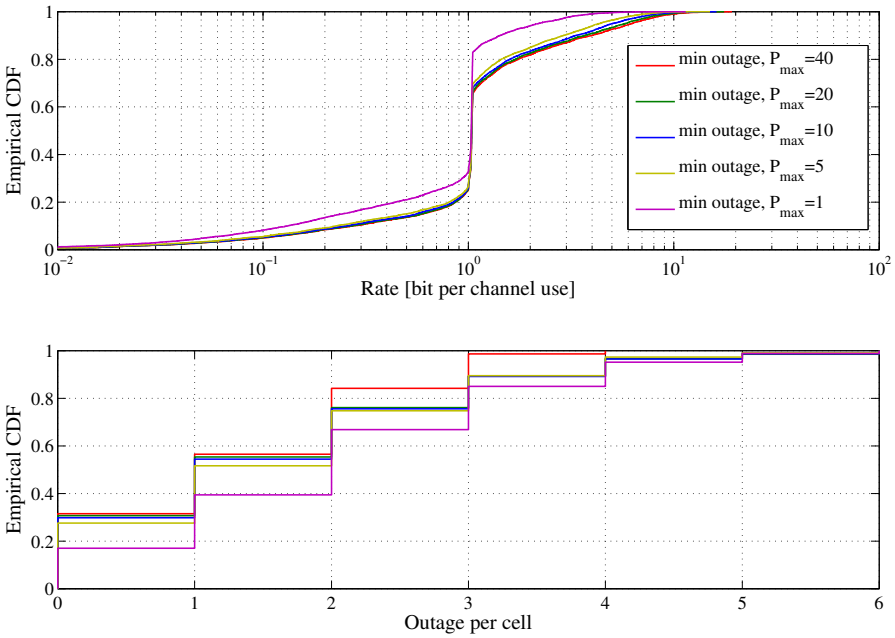

Figure 4.11: Results of applying Minimize Outage with different transmit powers.

It can also be seen that the performance drops radically if the BS power available is smaller than 5 W, this happens because then, the power at the BS may not suffice to transmit the signal to the corresponding BS for an average channel.

Chapter 5

Advanced Relay Implementations

The schemes developed in Chapter 4 can be applied to more sophisticated transmit schemes and more advanced relays. In the next section, one type of more complex AF relays is presented.

5.1 1-Way AF Relays with Matched Filter

So far, we have considered spatially white AF relays that multiply the incoming signal by the scaled identity and then forward the amplified signal. The performance of relaying can be increased by applying gain matrices that shape the channel in a beneficial way. To this end, $\mathbf{G}$ can be chosen to be the product of the transmit filter $\mathbf{G}_{\mathrm{TX}}$ and the receive filter $\mathbf{G}_{\mathrm{RX}}$,

$$\mathbf{G} = \mathbf{G}_{\mathrm{TX}} \cdot \mathbf{G}_{\mathrm{RX}},$$

where $\mathbf{G}_{\mathrm{TX}}$ is chosen to be a transmit matched filter for the RS-MS channel,

$$\mathbf{G}_{\mathrm{TX}} = \mathbf{F}^{H}.$$

This results in the M_{M} singular values of the channel to be squared. The receive filter reduces the M_{R} dimensional incoming signal to a M_{M} dimensional signal that can be multiplied by $\mathbf{F}^{H}$. $\mathbf{G}_{\mathrm{RX}}$ is designed to project $\mathbf{y}^{(R)} \in \mathbb{C}^{N_{\mathrm{R}}\mathrm{x}1}$ onto the M_{M} dimensional subspace with the fewest interference. This is performed by calculating the interference covariance matrix $\mathbf{K}_{\mathrm{i}}$ at each relay as

$$\mathbf{K}_{\mathrm{i}}^{(c,k)} = \sum_{\substack{b=1 \\ b \neq c}}^{N_{\mathrm{B}}} \mathbf{H}_{k}^{(c,b)} \mathbf{H}_{k}^{(c,b)\,H}$$

and choosing the M_{M} streams with the smallest eigenvalues. The columns of $\mathbf{G}_{\mathrm{RX}}$ are chosen to be the normed eigenvectors $\mathbf{v}_1, ..., \mathbf{v}_{M_{\mathrm{M}}}$ of $\mathbf{K}_i$ corresponding to the M_{M} smallest eigenvalues,

$$\mathbf{G}_{\mathrm{RX}} = \left[\mathbf{v}_1, \mathbf{v}_2, ..., \mathbf{v}_{M_{\mathrm{M}}}\right].$$

Relay power control for the AF relays with matched filter can be performed analogously to the spatially white case. In order to get a desired power $P_{\mathrm{RS}_i^{(c)}}$, we choose $\mathbf{G}_{c,i} = \beta_{c,i} \cdot \mathbf{G}_{c,i}^{(0)}$,

where

$$\beta_{c,i} = \sqrt{\frac{P_{\mathrm{RS}_i^{(c)}}}{\mathrm{Tr}\left\{\mathrm{E}\left[\mathbf{G}_{c,i}^{(0)}\mathbf{y}_{c,i}^{(\mathrm{R})}\mathbf{y}_{c,i}^{(\mathrm{R})H}\mathbf{G}_{c,i}^{(0)H}\right]\right\}}}. \tag{5.1}$$

The matrix $\mathbf{G}_{c,i}^{(0)}$ describes the original gain matrix without applying any power control.

In the next section, the power control algorithms ellaborated in Chapter 4 are applied to these more sophisticated relays and performence is compared to the spatially white relays.

5.1.1 Simulation Results

Figure 5.1 shows the results of minimizing power by applying Algorithm 2 to the different relay types. The red curves show the results for the spatially white AF relays and the blue curves the results for AF relays with matched filter. The dashed lines illustrate the results for applying power control and the solid lines show the results achieved without power control. Figure 5.1 shows that by applying power control in order to minimize power as described in Section 4.2.5 an average transmit power reduction from 2.73 W to 1.52 W per relay can be achieved by using the better AF relays. It can also be observed, that the better relays offer a larger potential of improvement through power control.

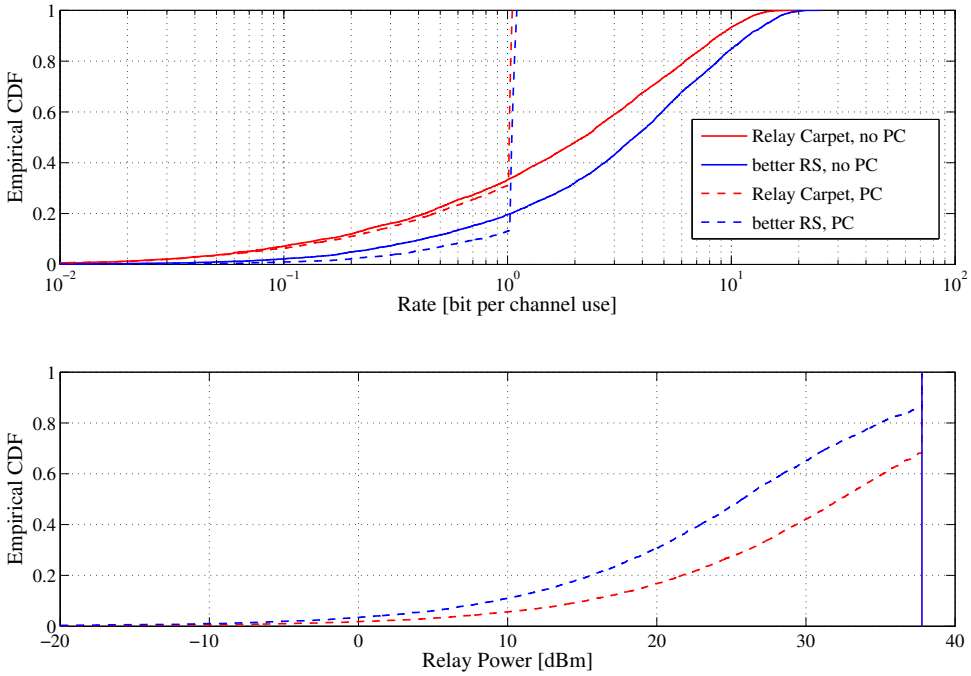

Figure 5.1: Minimize power for spatially white AF relays (red) and AF relays with MF (blue).

In Figure 5.2 CDFs of the achievable rates are shown that result from applying Algorithm 7 that aims to minimize the outage, as described in Section 4.4. The following four setups are simulated: Power control in the conventional network, where the BS sum transmit power is

chosen to be 76 W that corresponds to the total power available per cell in the Relay Carpet (blue), power control in the conventional network with $P_{\mathrm{b,max}} = 40$ W as in the Relay Carpet (red), power control in the Relay Carpet with spatially white AF relays (green) and power control in the Relay Carpet with AF relays applying a MF (magenta). The average outage per cell can be read from Table 5.1, where additional to the four PC schemes, the values of the outage without applying power control are given for comparison.

It can be observed, that the AF relays with MF achieve a much better outage than the spatially white relays even without doing any power control and from Table 5.1 it can be read that the potential improvement in outage through power control grows with the complexity of the network.

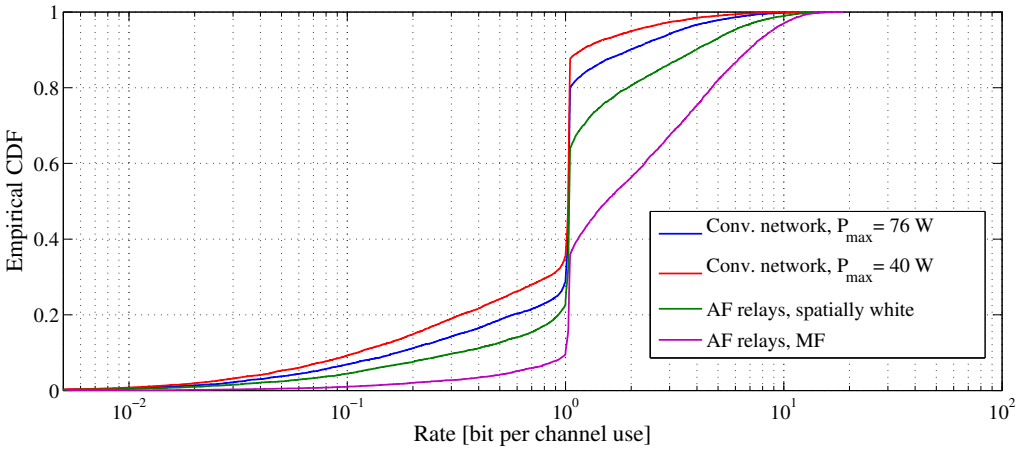

Figure 5.2: Minimize Outage for different types of relays.

	av. # outage per cell
Conv. network, $P_{\mathrm{b,max}}$=40 W, no PC	2.91
Conv. network, $P_{\mathrm{b,max}}$=76 W, PC	1.74
Conv. network, $P_{\mathrm{b,max}}$=40 W, PC	2.15
AF relays, spatially white, no PC	2.04
AF relays, spatially white, PC	1.37
AF relays, MF, no PC	1.15
AF relays, MF, PC	0.57

Table 5.1: Numbers to Figure 5.2

Chapter 6

Conclusion

We first introduced the concept of the Relay Carpet and pointed out its benefits over alternative approaches for wireless cellular networks. Results are shown that illustrate how performance can drastically be enhanced be the use of ubiquitous relays that can help to reduce the interference. Turning the cellular network into a two-hop network also simplifies CSI estimation at the terminals and allows for massive MIMO antenna arrays at the BSs.

In this thesis, power control and beamforming strategies that can be implemented in the promising Relay Carpet concept were elaborated. The problem of infeasibility that leads to divergence of the standard power control algorithms [8] is discussed and different approaches that guarantee convergence are found.

The developed schemes are able to improve performance in the network by generating less interference and adapting transmit power at the different nodes in order to achieve high data rates in an energy efficient manner. Simulation results have shown that large savings in power can be achieved, especially by choosing the right relays to be turned off and allocated to a different resource block. Further, we have illustrated the big improvements in outage that can be reached by allocating the total available power in a sophisticated manner. Base station power control schemes not only turned out to perform slightly better than RS control schemes, but are also easier to implement in practice, as large computations are performed at the BS. For the assumption of perfect CSI knowledge at the base station, BS power control can be performed by computing the optimum power allocation at each BS using the algorithms presented. In case of relay power control, computations are also performed at the BS and then, this information has to be transferred to the relays which leads to higher complexity. Alternatively to requiring the knowledge of the optimum power allocation at the relays, power control can be performed using feedback information on the achievable rate from the mobiles. Starting from an initial power distribution, power can then iteratively be adapted based on the actual rate at the corresponding mobile, according to the different schemes developed. This approach, however, leads to increasing complexity with the size of the network as iterations over the whole carpet are needed in order to converge to the optimal solution. But nevertheless, the promising results of the joint optimization schemes that clearly outperform BS optimization show that restricting power control to the BS is suboptimal. This asks for a more scalable implementation of the relay power control schemes that are realizable in practical cellular networks. A possible approach to solve the problem in scalability of the relay power control schemes presented in this thesis could be a distributed implementation of the relay power control algorithm. As interference is mainly caused by

nodes within the close vicinity and the influence of nodes that are located further away is negligible, solving the optimization locally is not expected to lead to a remarkable decrease in performance.

Overall, it has been shown that the performance of the Relay Carpet can significantly be improved by implementing power control schemes. The comparison of different types of relays has illustrated that implementing slightly more advanced relays and transmission schemes offers a larger potential of improvement through power control. Future versions of the Relay Carpet can thus highly benefit from applying power control.

Bibliography

[1] J. Lee *et al.*, "Coordinated multipoint transmission and reception in LTE-Advanced systems," *IEEE Comm. Mag.*, vol. 50, no. 11, pp. 44–50, Nov 2012.

[2] H. Huh, G.Caire, H.Papadopoulos, and S. Ramprashad, "Achieving 'massive MIMO' spectral efficiency with a not-so-large numberof antennas," *Wireless Communication, IEEE Transactions*, vol. 11, no. 9, pp. 3226–3239, 2012.

[3] A. Ghosh *et al.*, "Heterogeneous cellular networks: From theory to practice," *IEEE Comm. Mag.*, vol. 50, no. 6, pp. 54–64, June 2012.

[4] D. Gesbert *et al.*, "Multi-cell MIMO cooperative networks: a new look at interference," *IEEE JSAC*, vol. 28, no. 9, Dec. 2010.

[5] M. K. Karakayali, G. J. Foschini, R. Valenzuela, and R. Yates, "On the maximum common rate achievable in a coordinated network," *IEEE International Conference on Communications (ICC)*, June 2006.

[6] S. Ramprashad, G. Caire, and H. C. Papadopoulos, "Cellular and network MIMO architectures: MU-MIMO spectral efficiency and costs of channel state information," *Asilomar Conference on Signals, Systems and Computers 2009*, Nov. 2009.

[7] R. Rolny, M. Kuhn, and A. Wittneben, "The relay carpet: Ubiquitous two way relaying in cooperative cellular networks," Sep. 2013, accepted for publication at PIMRC 2013, London, UK.

[8] M. Chiang, P. Hande, T. Lan, and C. W. Tan, *Power control in wireless cellular networks*, June 2008.

[9] D. Tse and P. Viswanath, *Fundamentals of Wireless Communication*. Cambridge, 2008.

[10] A. Wittneben, "Lecture notes: Digital communication and signal processing," *ETH*, Spring Semester 2013.

[11] T. M. Cover and J. A. Thomas, *Elements of Information Theory (Wiley Series in Telecommunications and Signal Processing)*. Wiley-Interscience, 2006.

[12] I. E. Telatar, "Capacity of multi-antenna gaussian channels," *Eur. Trans. Telecommun.*, vol. 10, pp. 585–595, 1999.

[13] M. Costa, "writing on dirty paper," *IEEE Trans, Inform. Theory,*, pp. 349–441, May 1983.

[14] Q. H. Spencer, A. L. Swindlehurst, and M. Haardt, "Zero-forcing methods for downlink spatial multiplexing in multiuser MIMO channels," *IEEE Trans. Signal Processing*, vol. 52, no. 2, pp. 461–471, Feb. 2004.

[15] B. Rankov and A.Wittneben, "Spectral efficient signaling for half-duplex relay channels," *Signals, Systems and Computers*, 2005.

[16] M. Kuhn, R. Rolny, A. Wittneben, and T. Zasowski, "The potential of restricted PHY cooperation for the downlink of LTE-advanced," *IEEE Vehicular Technology Conference (VTC Fall)*, Sep. 2011.

[17] X. Mingbo, N. Shroff, and E. Chong, "A utility based power-control scheme in wireless cellular systems," *IEEE/ACM Transactions on Networking*, vol. 11, no. 2, pp. 210–221, April 2003.